SAN-1459-4
Distribution Category UC-63e

CADMIUM SULFIDE/COPPER SULFIDE HETEROJUNCTION CELL RESEARCH

Technical Progress Report #4
28 September 1978

1 June 1978 - 31 August 1978

Contract No. EG-77-C-03-1459

Electro-Optics
Electronics and Communication Sciences
Lockheed Palo Alto Research Laboratory
LOCKHEED MISSILES & SPACE COMPANY, INC.
Palo Alto, California 94304

ABSTRACT

The multi-cathode deposition system has been brought into operation and used to deposit multilayer films of Cu_xS/CdS/In/Al in a single pumpdown. In addition, it has been used to prepare In doped CdS films by co-sputtering of Cd and In. Analysis of the photovoltaic devices deposited in the system to date have determined the areas requiring further development. These are the CdS/substrate contact and the doping distribution through the CdS film. The initial photovoltaic cells have been characterized by a built in retarding field. Electrical, optical and structural measurements on all components of the multilayer films have been carried out and related to the corresponding deposition parameters. The theory of reactive sputter deposition of compound semiconductors has been developed to explain the rate limiting deposition processes and the ease with which a stoichiometric compound is formed.

INTRODUCTION - SUMMARY

Objective

The program objective is to investigate and evaluate the application of cylindrical-post magnetron reactive sputtering to the production of solar cell quality thin films of CdS/Cu_2S for large scale terrestrial photovoltaic energy conversion.

Emphasis for This Quarter

A primary objective during this quarter was to complete the assembly of the multi-cathode deposition system and to conduct shakedown tests. This objective has been completed and the system is now being used to deposit multi-layer coatings. The versatility of the apparatus has also been used to deposit In-doped CdS coatings by co-deposition.

A second major emphasis has been to deposit coatings of CdS with controlled resistivity levels. The desired resistivity range is very low compared to that of stoichiometric CdS (1 to 10Ω-cm). The initial approach was to achieve the desired conductivity by depositing coatings with controlled departures in stoichiometry. This approach has proved to be difficult because of what are believed to be some fundamental aspects of the deposition process. Therefore the emphasis has been switched to the use of indium doping as a method for controlling the conductivity.

Cu_xS coatings have been deposited over the CdS coatings that were formed as part of the resistivity study. This was done as part of the shakedown of the multi-source deposition apparatus. It has also provided Cu_xS coatings that can be compared with the Cu_xS coatings that were deposited on glass during the preliminary studies described in Technical Progress Report No. 3 [1]. In addition, these Cu_xS/CdS heterojunctions provide an opportunity to begin preliminary photovoltaic barrier measurements.

All of the CdS coatings are being deposited over pre-deposited electrodes, which serve as rear contacts and assist in evaluating the electrical properties of the semiconductor layers. These rear contacts also permit evaluation of various electrode materials with respect to their ability to form ohmic contacts with the reactively sputtered CdS.

A final emphasis during this reporting period has been in preparing for the deposition of the gold grid electrodes so that test type solar cells can be fabricated. This activity has included preparing a gold sputtering target, substrate holders and deposition masks.

Activities for This Quarter

Activities during the fourth quarter reporting period were directed toward the following tasks:

- o Assembly of Specialized Deposition System (Task 1.1)
- o Deposition of $Cd_{1-x}Zn_xS$ (Task 1.2)
- o Substrate Contact (Task 1.3)
- o Structural Measurements of $Cd_{1-x}Zn_xS$ (Task 1.4)
- o Electrical Measurements of $Cd_{1-x}Zn_xS$ (Task 1.5)
- o Deposition of Cu_2S (Task 1.6)
- o Structural Measurements of Cu_2S (Task 1.7)
- o Electrical Measurements of Cu_2S (Task 1.8)
- o Photovoltaic Barrier Measurements (Task 1.9)
- o Au Grid Fabrication (Task 2.1)
- o ZnS Coating (Task 2.2)
- o Theoretical Analysis (Task 3)
- o Conversion Efficiency (Task 4)
- o Device Cost Projections (Task 5)

The assembly of the specialized deposition system is complete. Shakedown tests have also been completed. The system has been successfully used to fabricate all-vacuum heterojunctions.

The problem of fabricating the sputtering targets is believed to have been solved. Several methods have been successfully tested which can be used to fabricate cylindrical Cd sputtering targets with the desired 6-9's purity. A method involving direct casting of thick-walled targets without supporting structures has been selected. A Cd target of 6-9's purity that was formed in this way is presently in use. Targets composed of Zn and Cd-10% Zn are currently being cast at Cominco American.

An investigation has been made of the influence of the H_2S injection rate and the substrate temperature on the structural and electrical properties of CdS coatings formed by reactive sputtering in an Ar-H_2S atmosphere. Near stoichiometric coatings with high resistivities and Hall mobilities in the 1 to 10 cm^2/V-s range were found to deposit over a wide range of H_2S injection rates and substrate temperatures. It is believed that this strong tendency to produce near-stoichiometric coatings is due to a large flux of sulfur-bearing species which are generated at the cathode surface and make the cylindrical magnetron reactive sputtering process similar to the two-source, three-temperature method of evaporation.

The strong tendency of the reactive sputtering process to produce near-stoichiometric CdS suggests that the method may be very reliable for producing a host material for use with doping. A Cd-Zn (Zn-10% atomic percent) cathode with 200 ppm of In doping is currently being cast at Cominco American. Preliminary doping studies using co-deposition from In and Cd sputtering sources are underway. A reduction in the electrical resistivity with increasing In doping is observed.

Cu_xS films are being deposited over at least one of the CdS coatings which are being formed during each run in the CdS material studies described above. Thus the samples generated during a given run permit the properties of both the CdS and an associated heterojunction to be examined.

Electrical and photovoltaic properties of Au/CdS and Au/Cu_xS/CdS are being determined as a function of deposition parameters and bulk properties of the constituent layers. Schottky barrier measurements give the CdS surface doping density while heterojunction measurements give photovoltaic response characteristics. Photocurrent collection efficiency in Au/Cu_xS/CdS structures formed to date has been poor, apparently due to a retarding built-in drift field in the CdS.

SEM measurements of CdS surface topology and fracture cross sections along with x-ray diffraction pole figure determinations were carried out. The SEM investigation indicated the anticipated variation of growth habit with H_2S pressure at a substrate temperature of $T_s = 300^oC$. At low H_2S pressures, a dendritic structure was obtained and as H_2S pressure increased, the film crystallinity and density also increased. The pole figures indicated a preferential orientation of the CdS c - axis about 12^o off normal from the plane of the substrate.

Measured Cu_2S film absorption coefficients have been combined with the solar spectral irradiance to determine optimum Cu_2S film thickness and maximum short circuit currents obtainable in a planer structure.

Re-evaporation of Cd at elevated substrate temperatures results in a lower than anticipated rate of CdS film growth. However, the dense structure of the reactively sputtered CdS films allows use of a film only 2 to 3μm thick. Device cost projections have been computed using the experimentally determined CdS film deposition rates and thicknesses.

TECHNICAL DISCUSSION

Task 1.1 Assembly of Specialized Deposition System

The specialized deposition system is designed to locate four mangetron sputtering sources surrounding a rotatable substrate holder, as shown in Figure 1. The apparatus permits multi-layer coatings of various configurations to be deposited without breaking vacuum. Particular features of the system were described in Technical Progress Report No. 2.

Figure 2 shows a photograph of the chamber top plate taken during assembly. The magnetron sources are mounted in the top plate. The view in the photograph is from the right in Figure 1, looking left. Referring to Figure 2, the substrate holder with eight wafer positions is seen in the center. The magnetron for depositing the Cu_xS coatings is to the right of the substrate holder. Only its cylindrical outer shield is visible. The aluminum cathode with its shield removed is on the left.

The assembly of the specialized deposition system has been completed. Shakedown tests have also been completed. In its initial configuration Al, In, Cd, and Cu sputtering sources have been located at the four cathode positions. The Cd and Cu sources are being used to form Cu_xS/CdS heterojunctions. The In source is being used to deposit an overcoat on the rear contact electrode and for doping the CdS by simultaneously sputtering from both the Cd and In sources.

Task 1.2 Deposition of $Cd_{1-x}Zn_xS$

Target Fabrication Problem

Progress in the program has been delayed by difficulties in fabricating the high purity Cd and Cd-Zn sputtering rargets. These difficulties were discussed in Technical Progress Report No. 3 [1]. The initial plan was to cast the Cd over nickel-plated copper supports designed to give strength to the assembly, since Cd is a relatively soft and mechanically weak material. Attempts to fabricate the targets in this way were plagued by impurities which entered the high purity cast material from the supporting structure by diffusion. Three solutions ultimately evolved.

1) Pre-cast the sputtering targets. Then attach them to the support using a low melting point material. Some diffusion of the low melting point material into the casting will result. However this contamination level will be small compared to a typical doping level. Thus this method can be effectively used, with In as the low melting point bonding agent, for fabricating targets that are to be doped

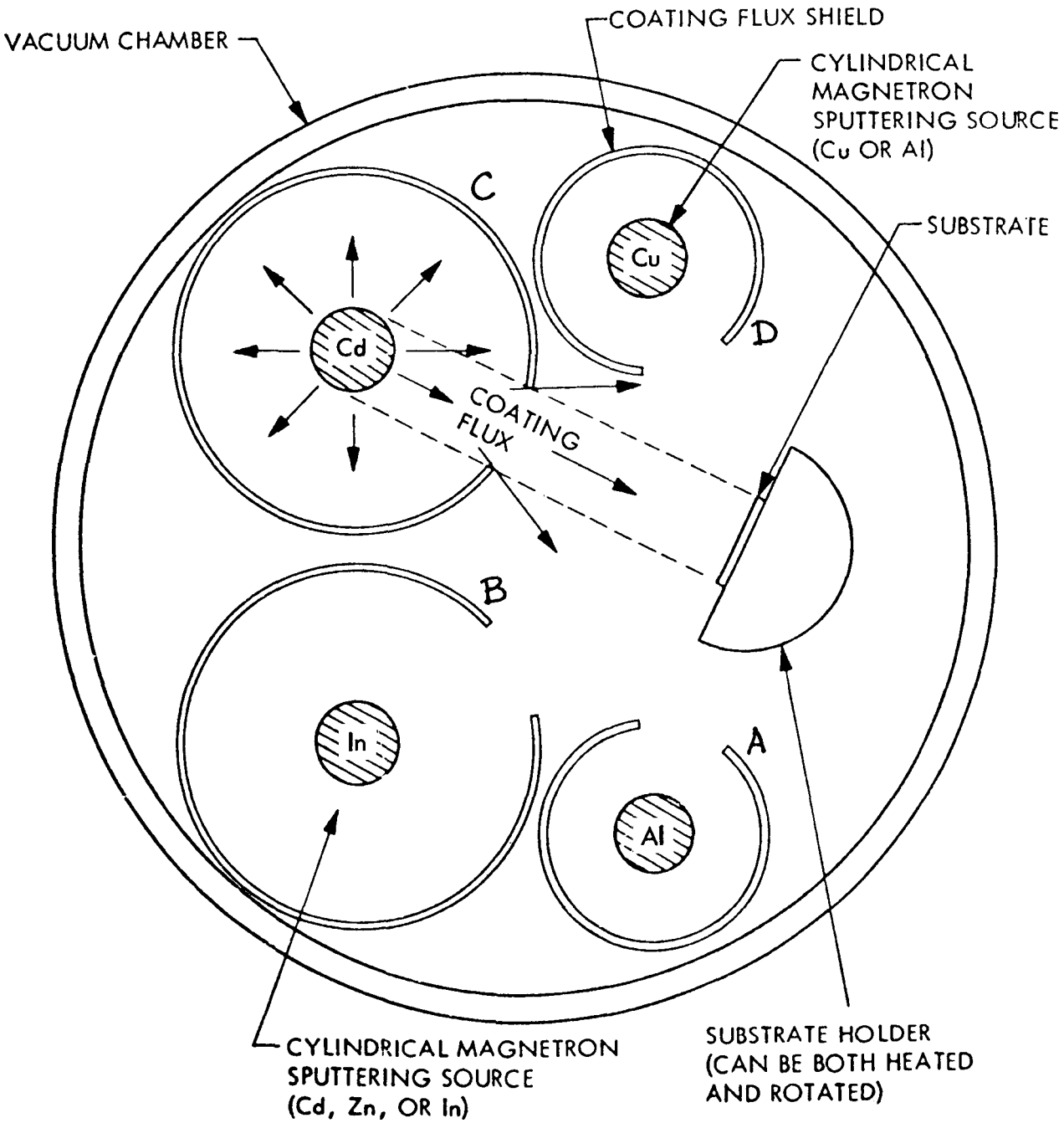

Fig. 1 Multicathode Magnetron Reactive Sputtering System Schematic for Sequential Deposition of Multilayer Films

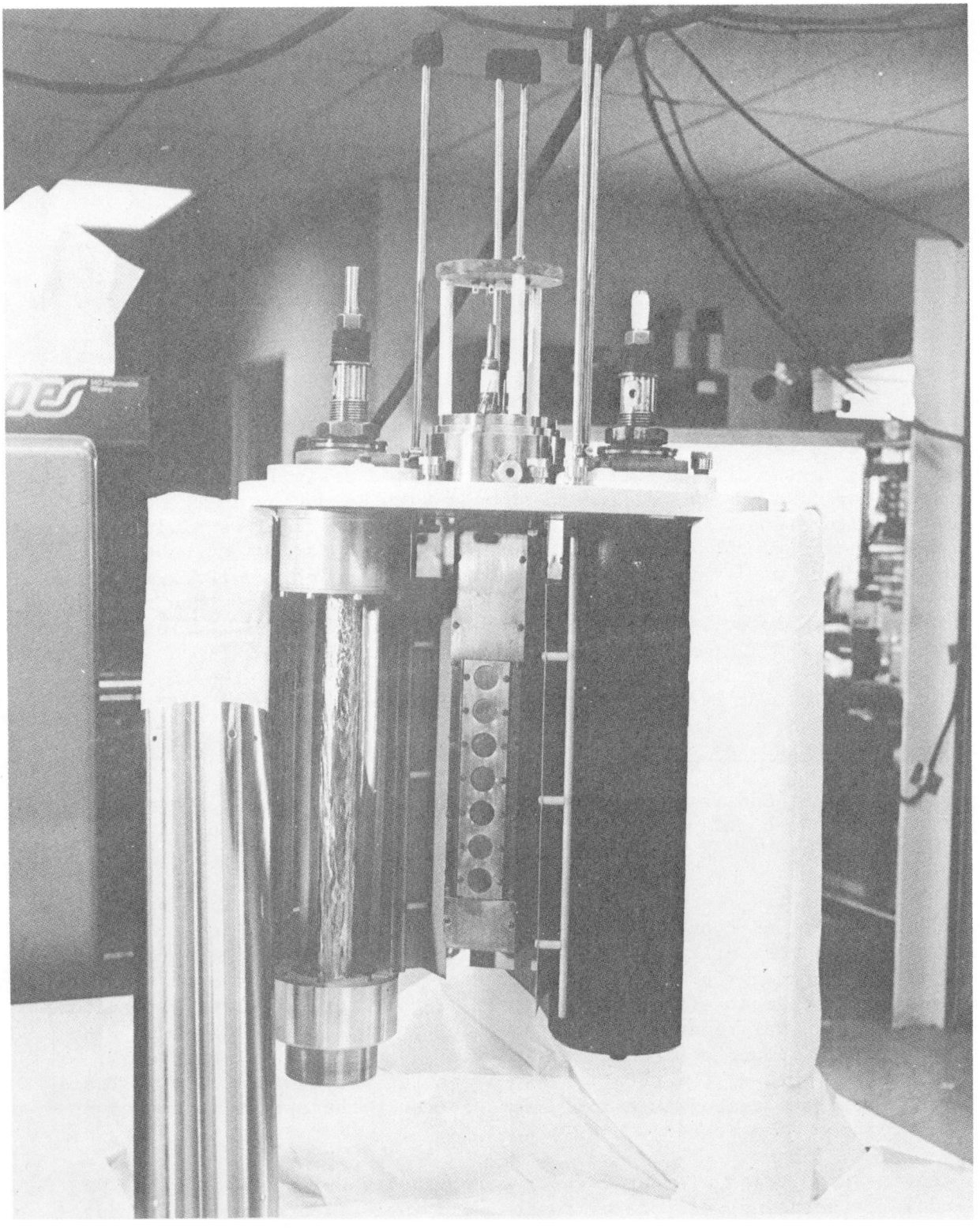

Fig. 2 Partially Assembled Multicathode Magnetron Reactive Sputtering System

with In (In doping for Cd and Cd-Zn targets is believed to be desirable for reactive sputtering - see next section.).

2) Pre-cast the sputtering targets as described in Item 1 above. Then attach them to the support using conducting epoxy (a common approach used in fabricating planar sputtering targets). Experiments at Cominco American using a Ag-based epoxy to attach pre-cast Cd to a Cu support yielded good bonding with no evidence of Ag or other contaminants passing into the Cd.

3) Cast targets of the desired purity with sufficient wall thickness and strengths so that backing supports are not required.

The thick-walled casting approach (#3) has been selected. A review of the magnetron mechanical design indicated that with some relatively minor modifications much of the stress could be removed from the sputtering target. A thick-walled Cd target of 6-9's purity was cast at Cominco American and successfully tested in a magnetron of the modified design. Cominco American is now preparing a Cd-10% Zn (atomic) target with In doping in the thick-walled configuration. Casting has been completed and final machining is currently underway. This target should be delivered during September. Cominco American will then begin casting a Zn cathode of the thick-walled configuration for use in forming anti-reflective coatings. By the time the Zn target is completed, it is anticipated that the $Cd_{1-x}Zn_xS$ studies with the doped target will have progressed to the point where the Zn and In compositions can be specified for a final target that is scheduled to be fabricated by Cominco American during the present program.

CdS Reactive Sputtering Studies

A first series of CdS reactive sputtering experiments in which the electrical properties of the coatings were examined as a function of the H_2S injection rate and substrate temperature have been completed.

Before reporting the results of these experiments it is useful to make some general observations concerning the substrate temperature, since it is perhaps the single most critical parameter in determining the structure and properties of coatings produced by the techniques of vacuum evaporation and sputtering. The gross effects of substrate temperature on coating structure are discussed in Reference [2]. In general, the grain size increases with temperature. Compound semiconductors present a special case, however, because one or more of the constituents are often very volatile [3]. Therefore the substrate temperature influences not only the structure but also the composition of a coating.

The condensation of an elemental vapor onto a solid surface is a function of complex adsorption, surface diffusion, and nucleation phenomena. Thus for given arrival flux, condensation sets in spontaneously below a critical temperature which depends on the arrival flux, the sticking coefficient, and the equilibrium vapor pressure. Figure 3 shows calculation of the

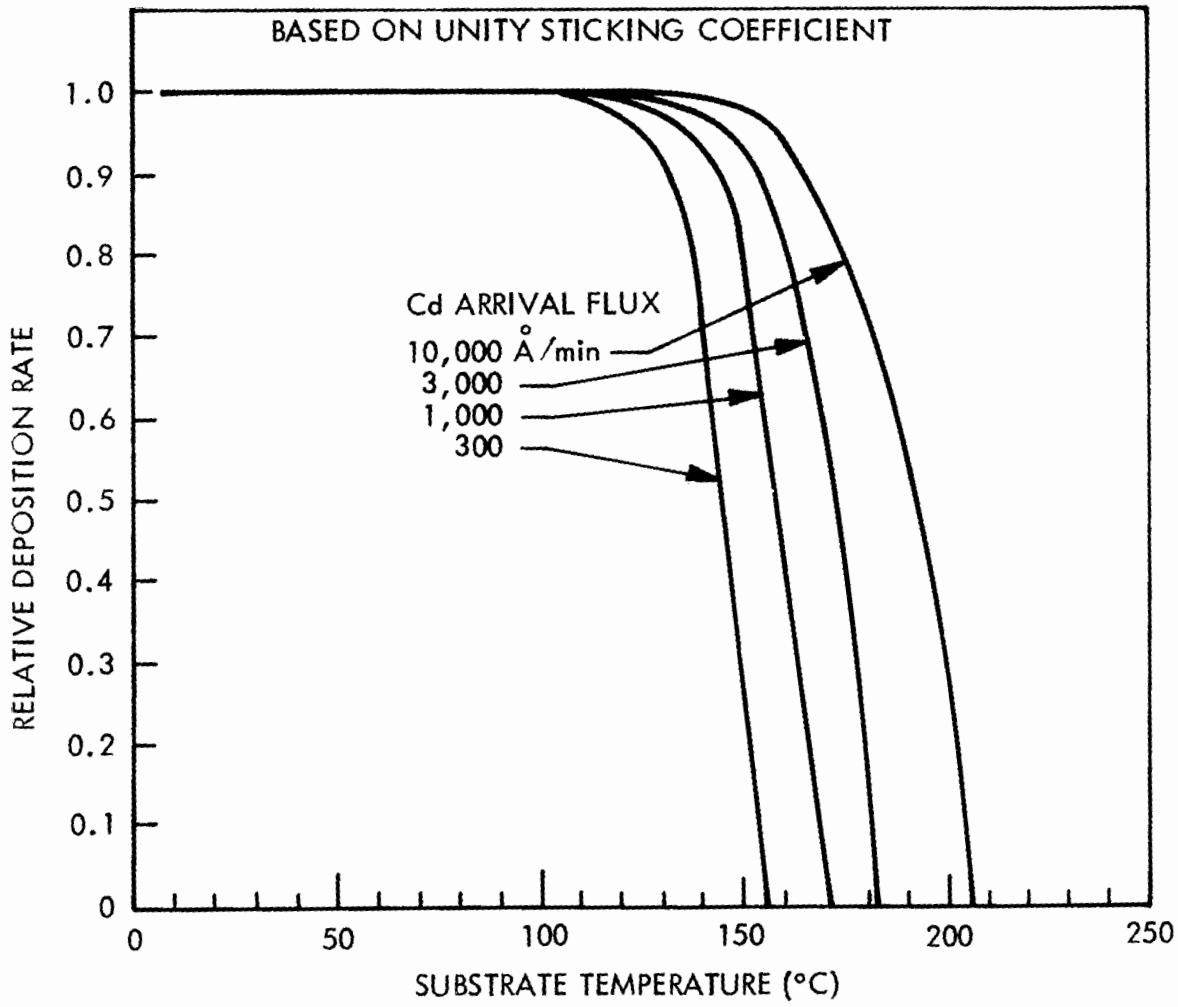

Fig. 3 Theoretical Deposition Rate for Cadmium as Function of Substrate Temperature. Based on Unity Sticking Coefficient

temperature dependence of the deposition rate for various arrival fluxes of Cd and an assumed unity sticking coefficient. Experimental measurements of the sputtered Cd flux have been found to be consistent with this picture but imply a sticking coefficient of less than one for Cd deposition on glass and aluminum surfaces. Thus a very rapid drop in deposition rate was found for an arrival flux of 1000 Å/min when the substrate temperature exceeded about 140°C. No deposit was found on glass or aluminum coated surfaces which were exposed to the sputtered Cd flux for 5 min. at a substrate temperature of 160°C.

If two different elemental vapor streams are incident on a common substrate, then the condensation and re-evaporation of each, as well as the reaction between them, needs to be taken into account. In a temperature range in which the compound formed by the constituents is stable, the interaction between the two species on the substrate causes the condensation coefficient of each to be increased by the prssence of the other. This is the basis of the three-temperature method for forming stoichiometric compounds by multi-source evaporation.

In the three-temperature method the source temperatures are maintained such that the evaporated flux is rich in the more volatile constituent (S in the CdS case). The substrate temperature is maintained above the critical condensation temperature for the volatile species but below the dissociation temperature of the compound. If the flux of volatile material is large enough, surface reactions will consume all of the less volatile material (Cd in the CdS case) to form the compound. The deposition process is therefore rate limited by the arrival rate of the less volatile material. The fraction of the more volatile species which does not react is re-evaporated from the substrate so that only the stoichiometric compound survives.

When CdS is sublimed from an open crucible, the flux tends to be deficient in sulfur [4]. At low substrate temperatures (<150°C) the excess Cd condenses and is incorporated into the coating as quenched-in interstitial Cd or as metallic precipitants. The coatings are dark in color and highly conducting. At substrate temperatures above about 200°C, much of the excess Cd is re-evaporated, yielding yellow coatings with much higher resistivities. Thus the substrate temperature is often used to control the conductivity of evaporated coatings. With the addition of a second source to provide a simultaneous evaporation of S, high resistivity near-stoichiometric CdS coatings can be formed at room temperature.

Now consider the reactive sputtering case. It has been noted in previous reports [5] that the reactive sputtering process in general, and Cd-Ar-H_2S reactive sputtering in particular, is characterized by two modes of operation. In one "metal" mode, at low H_2S injection rates, the primary process is Ar sputtering of metal and the coatings tend to be metallic in nature. In the second "dielectric" mode, at higher injection rates, the coatings tend to be stoichiometric in nature. The mode transition is illustrated in Figure 4. Curve A is the total pressure (H_2S + Ar) in the coating chamber in the absence of sputtering. This pressure results from a balance between the rate

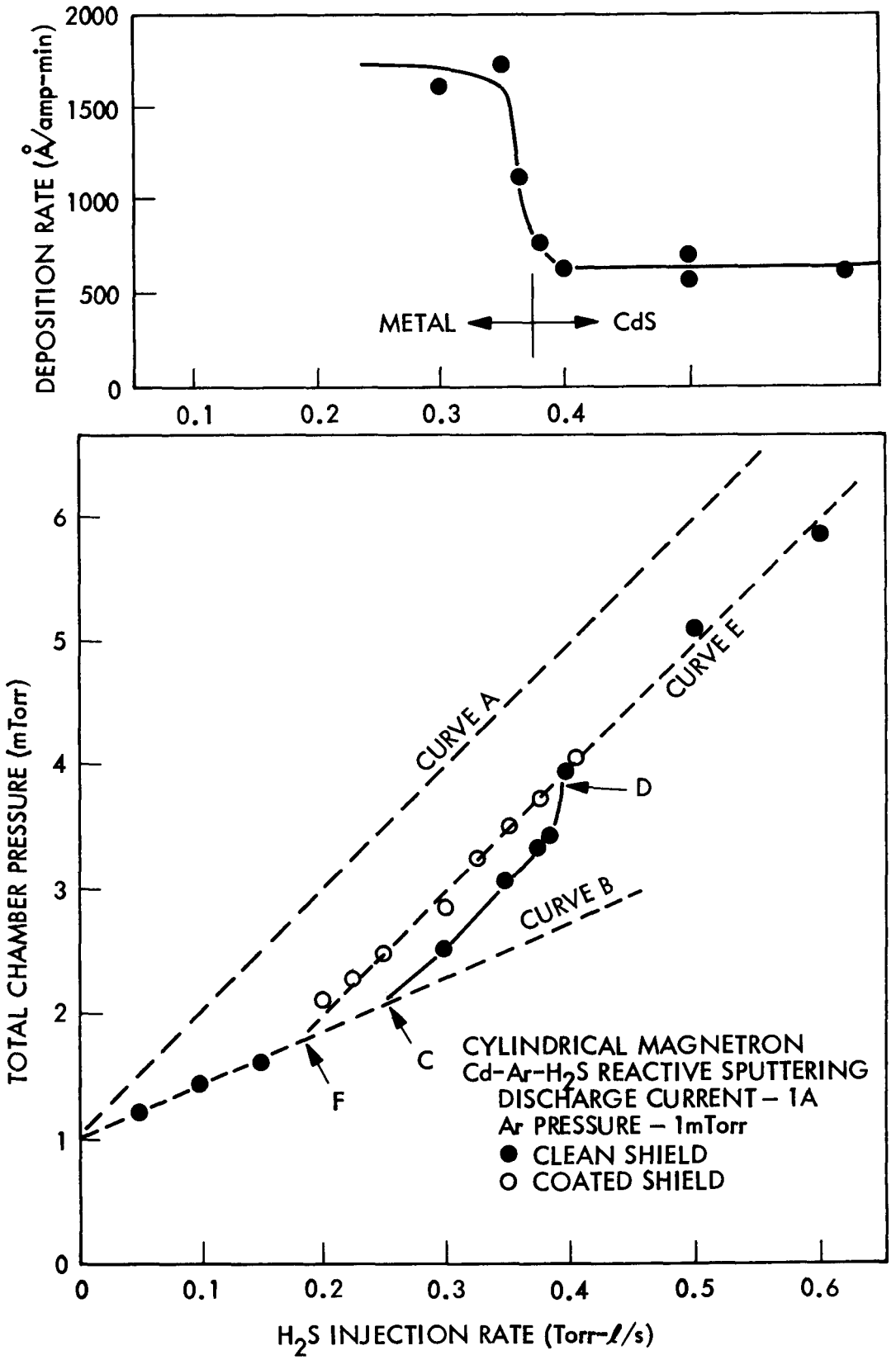

Fig. 4 Variation of Sputter Chamber Pressure and Deposition Rate With Reactive Gas Injection Rate for CdS Film Formation

of H_2S injection and the chamber pumping speed. Curve B corresponds to the case where the injected H_2S is totally consumed by the sputtering process with the release of H_2 (see Technical Progress Report No. 2 [5]). Note that the experimental data with the sputtering discharge in operation follow this curve. It is believed to be the gettering action of the depositing Cd which incorporates the S. However, the coatings deposited along curve B are metallic in nature. As the sulfur content of the depositing coating increases, the coatings' efficiency for incorporating additional S decreases, and the operating curve breaks away at point C. However, the coatings deposited on low temperature substrates and on the shields which surround the source (see Fig. 1) are still metallic in appearance and electrically conducting, although the resistivity is much larger than that of bulk Cd. The mode transition occurs at D. The transition is believed to occur because the efficiency of incorporating H_2S into the growing coating drops significantly as the coating composition approaches the stoichiometric value. Thus the getter pumping efficiency on the surface surrounding the cathode drops, and the H_2S partial pressure in the coating chamber rises. This pressure rise changes the composition of the gas within which the sputtering discharge is maintained from primarily Ar to an Ar-H_2S mixture. The result is a complete change in the nature of the sputtering mechanisms. They change from a case in which a relatively clean metal surface is being sputtered by argon (metal mode) to a case in which the target surface becomes modified, with the result that an intense flux of reactive species (primarily sulfur atoms and H_2S molecular fractions) is produced at the cathode and accompanies the sputtered metal to the substrates (dielectric mode). A reduction in deposition rate also occurs at the mode transition, as shown by the upper curve in Figure 4. Beyond point D the operating pressure follows curve E, which is parallel to curve A, since the coatings are nearly stoichiometric in nature and no additional H_2S can be consumed.

The data discussed above are for experiments in which the deposition surfaces surrounding the cathode are relatively clean. Often the operating state of a reactive sputtering system is dependent on the initial state of the surrounding surfaces. This has been found to be the case for Cd-H_2S reactive sputtering. As shown in Figure 1, the shields constitute the major deposition surface that surrounds the cathode. Thus it has been found that the transition point moves from D to F as CdS is accumulated on the shields over many hours of operation. This latter point has been confirmed by observing the variations in system performance as wall shields that had become heavily coated were removed, then replaced, then removed again and cleaned and finally replaced again.

The large flux of sulfur-bearing species makes the cylindrical magnetron reactive sputtering process similar to the two-source three-temperature method of evaporation described previously. In particular, the Cd arrival rate is rate-limiting as long as the H_2S injection rate is sufficiently large to provide adequate S to convert all of the Cd on the substrate surface to CdS. This is the case in the dielectric mode. Thus, in the experiments referred to above, it has been observed that as the substrate temperature is increased the CdS accumulation rate decreases, probably because the rate-

limiting Cd deposition rate is decreased by evaporation. The effect is shown in Figure 5.

Now if the H_2S injection rate is decreased so that there is insufficient sulfur to react with the Cd, then a metallic coating will form on a cold substrate (operation in metal mode). However, if the substrate is at an elevated temperature, the excess Cd will evaporate and the sulfur will become the rate-limiting step. This behavior is shown in Figure 6.

The experiments performed thus far indicate that near-stoichiometric coatings with high resistivities are produced under a wide range of H_2S injection rates and substrate temperatures; i.e., under conditions where either the S flux or the Cd flux is rate limiting. Achievement of conductivity contorl by forming Cd-rich CdS requires that the sputtering apparatus be operated in the metal mode to provide excess Cd in the arriving coating flux, and that the substrate temperature be low enough to suppress the loss of excess Cd by evaporation and yet provide the desired conductivity. Required substrate temperatures are in the range 140 to 200°C, depending on the Cd arrival rate. A high Cd sputtering rate is desired for this approach. Most of the work thus far has been with dc power applied to the cathode. With this form of operation, current densities and sputtering rates have been limited by arcing (see Technical Progress Report No. 2 [5]). However, we have demonstrated that high rates can be achieved using rf power. Preliminary experiments have been conducted in which coatings which are designed to have graded Cd/S compositions were deposited by varying the H_2S injection rate and the substrate temperature during the course of the deposition. Coatings with reduced resistivities have resulted. However, adhesion has been poor. Additional work is planned. This general approach is complicated by the influence of the chamber walls (shield surfaces) on the dielectric mode transition point as discussed above.

The strong tendency of the Cd-H_2S reactive sputtering process to produce stoichiometric coatings at elevated substrate temperatures suggests that doping should be very effective in providing control over the CdS conductivity. The ability to control the doping level is one of the advantages of the sputtering process. The reactive sputtering should provide a host material that is relatively insensitive to minor variations in the deposition conditions. Thus Cominco American has been instructed to incorporate 200 ppm of In into the Cd-10% Zn target which they are preparing for use in the $Cd_{1-x}Zn_xS$ studies.

Co-deposition is being used to explore the effects of indium doping on the conductivity of the CdS coatings while awaiting delivery of the doped target. An In cylindrical magnetron sputtering target has been placed at one of the positions adjacent to the Cd target, as shown in Figure 1. The In flux is somewhat non-uniform over the substrate and arrives at an oblique angle. However the configuration is believed to be adequate for preliminary experiments. A series of CdS coatings deposited with various fluxes of In have been prepared. Preliminary coatings of a graded nature in which the In flux or the substrate temperature was varied during the deposition have also

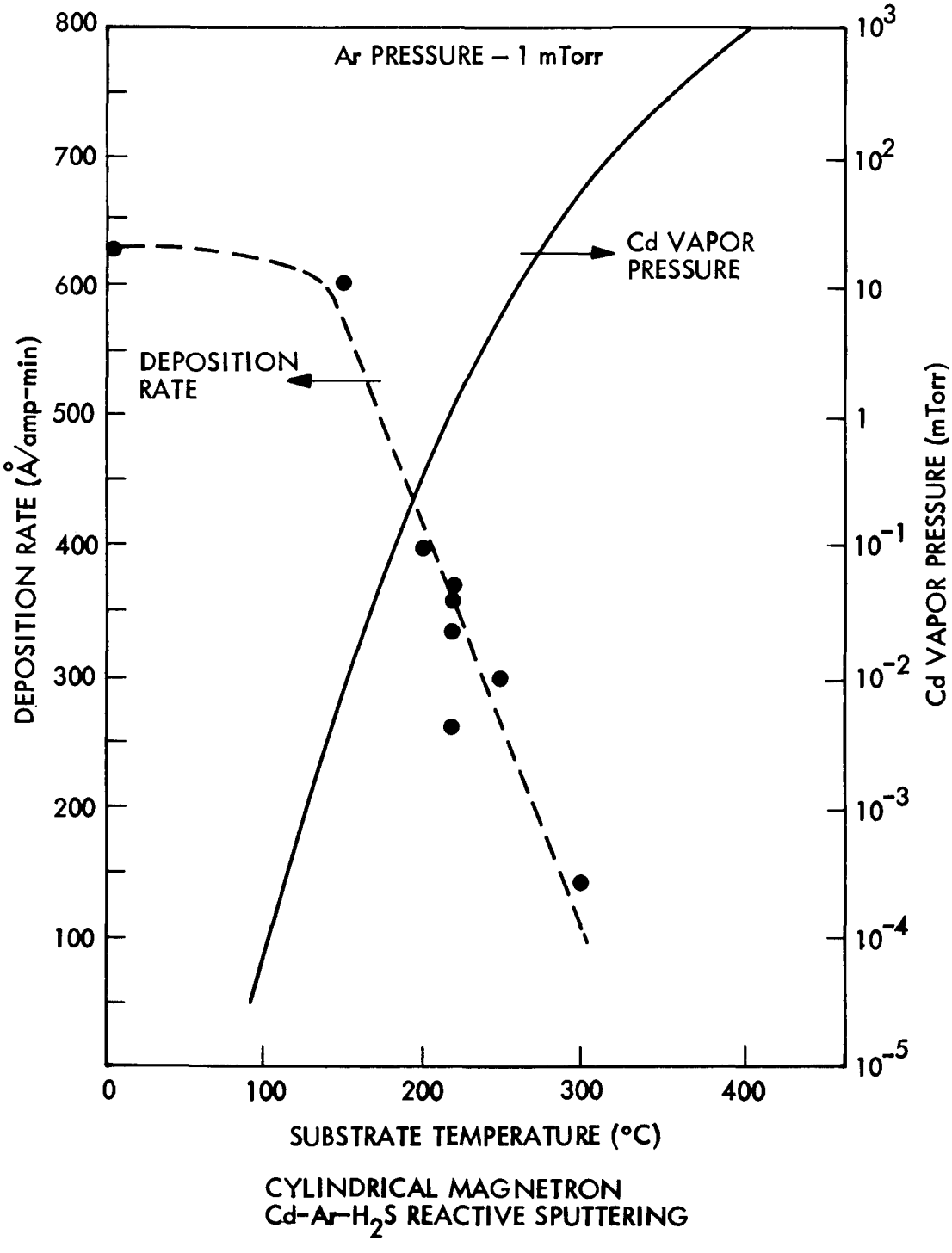

Fig. 5 Comparison of CdS Deposition Rate Versus Substrate Temperature With Cd Vapor Pressure (Over Cd) Versus Temperature

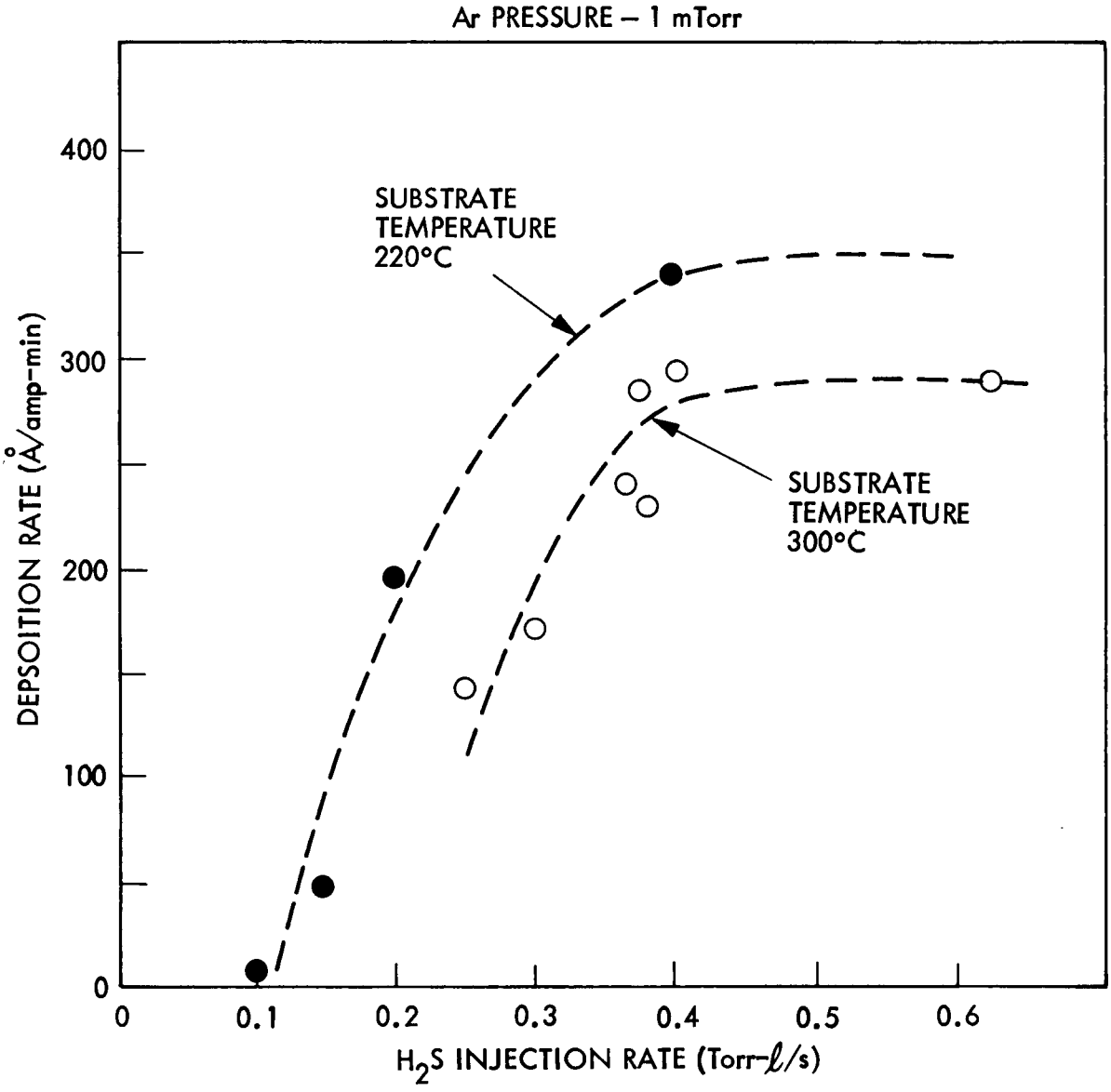

Fig. 6 Parametric Dependence of CdS Deposition Rate on H_2S Injection Rate and Substrate Temperature

been prepared. Note that because of the low vapor pressure of In, an elevated substrate temperature produces an increase in the In relative to the Cd composition for a deposit formed from a coating flux of given composition.

Adhesion and Internal Stress

Good adhesion has been found at all substrate temperatures for CdS coatings deposited onto plates with pre-deposited metal electrodes or indium-tin-oxide layers. However, CdS coatings deposited on borosilicate glass substrates at temperatures of less than about 300°C have exhibited poor adhesion. The adhesion problem on the glass substrates is somewhat academic, since the CdS will be deposited over metal electrodes in forming the solar cells. However, the poor adhesion is a possible sign of internal stresses within the coatings. Representative CdS and Cu_xS coatings were deposited on calibrated glass wafers for purposes of measuring the stress levels, as discussed in Technical Progress Report No. 3 [1]. An analysis of the internal stress in the Cu_xS samples has been completed. The results are shown in Figure 7 along with comparative data for metallic chromium deposited by sputtering under conditions (low and high Ar pressures) that yielded high compressive and high tensile stresses. The vertical scale is the force at the interface or the stress integrated through the coating thickness. It is seen that the stress in the Cu_xS is tensile and of relatively low magnitude.

Task 1.3 Substrate Contact

The CdS coatings described in the preceding section are being deposited through masks which yield 1.9 cm disk patterns for the semiconducting deposits, as shown in Figure 4a of Reference [5]. The pre-deposited rear contact electrode covers the entire 2.5 cm x 2.5 cm borosilicate substrate. Some CdS coatings were deposited over Nb rear electordes. However most of the work has been done using Al electrodes deposited after plasma cleaning the substrates, as described in Technical Progress Report No. 2 [5].

The aluminum sputtering source was included in the specialized deposition system so that a fresh aluminum layer could be deposited over the pre-deposited aluminum in order to neutralize the oxide layer. It was found that CdS coatings deposited over the pre-deposited aluminum (without the fresh Al layer) did indeed yield non-ohmic contacts. The deposition of a 300 Å layer of fresh aluminum as a first step in the CdS deposition did not improve the contact. Subsequent CdS coatings have been deposited with a thin indium layer over the pre-deposited aluminum. CdS coatings with In layer thicknesses of about 150 Å, 500 Å and 1000 Å have been prepared.

Diodes (both Schottky and heterojunction) formed on CdS with 150 Å of In undercoated had satisfactory rectification characteristics. Diodes formed on CdS with 500 Å or 1000 Å of In undercoated typically had soft reverse breakdown characteristics. Further work is required to establish ohmic contact between the CdS and substrate.

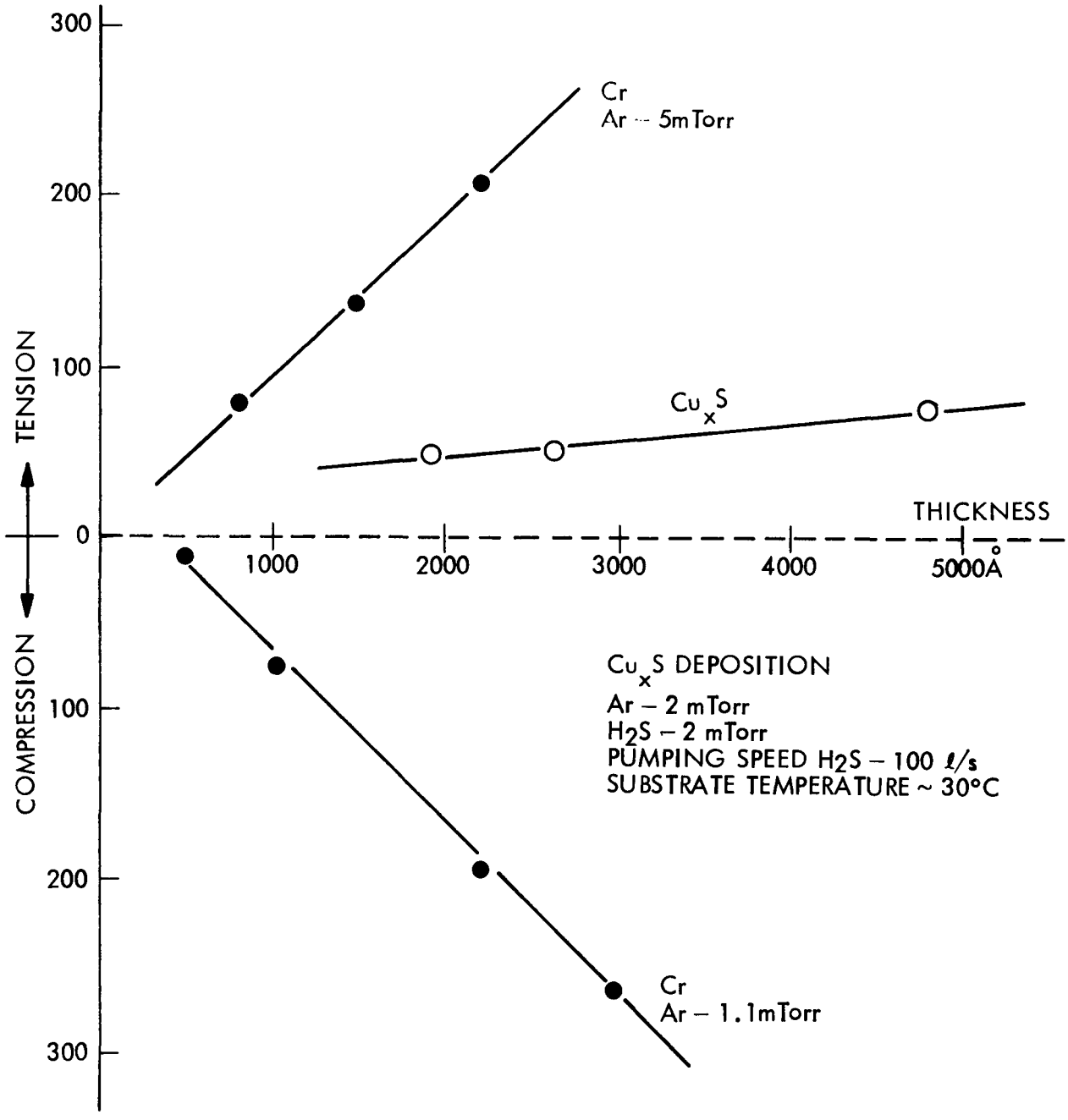

Fig. 7 Force Per Unit Width at Interface as Function of Coating Thickness for Cu_xS coatings Deposited by Reactive Sputtering. Comparative Chromium Data from Reference 4. Internal Stress is Proportional to Slope of Force Per Unit Width Curves

Task 1.4 Structural Measurements of $Cd_{1-x}Zn_xS$

The structural changes in CdS films deposited at various H_2S partial pressures are shown in the SEM photos of Figure 8. All these films were deposited onto a glass substrate at $T_s = 300^oC$ and with an Ar partial pressure of 1.0 mTorr. From the fracture cross sections (top row of Fig. 8), the film structure appears to change from a fibrous or columnar structure to a denser, equiaxed grain structure as the H_2S partial pressure is increased. This structural change is also apparent as increased surface faceting in the top surface SEM views (bottom row of Fig. 8).

All of the film structures in Figure 8 are quite dense, i.e. no open boundaries which can result in top surface contact shorts to the substrate. Electrical measurements, to be described in the next section, indicate that CdS film integrity is such that reactively sputtered CdS films of 2.0 to 3.0μm thickness are satisfactory for thin film cells.

Preferred orientation of a reactively sputtered CdS film is with the basal plane inclined to the substrate plane as indicated in Figure 9. The numbers represent the number of times greater than a random distribution the 0001 pole is oriented in a particular direction. As the substrate temperature is reduced, the preferred orientation distribution broadens and moves further off axis. Figure 9 indicates a preferred orientation of the 0001 pole about 12^o inclined with respect to a normal to the substrate.

Task 1.5 Electrical Measurements of $Cd_{1-x}Zn_xS$

Both Schottky barriers (Au/CdS) and heterojunctions (Cu_xS/CdS) have been formed on the CdS films to evaluate the electronic properties of the films. An array of 9 Au circles, 2 mm diameter spaced on 5 mm centers, is vacuum evaporated onto the 19 mm diameter CdS (or Cu_xS/CdS) circles. Thus the Au contact area covers 10% of the film area. For CdS films 3μm thick, there are typically no shorts of the Au contact through the CdS film to the substrate.

A typical Schottky barrier current-voltage and $1/C^2$ -voltage curve for a 3μm CdS film is shown in Figure 10. Superimposed on the $1/C^2$-voltage plot is an ionized impurity plot obtained by assuming all of the capacitance change is due to changing space charge density at the boundry of the space charge region-neutral bulk region. In fact, some of the change in space charge density may be due to deep levels near the surface. In either case, a nominal surface carrier density of $\sim 2 \times 10^{16}$ cm^{-3} is indicated. However, the high forward resistance of the Schottky diode indicated in Figure 10a implies a bulk resistivity of $\rho \gtrsim 7 \times 10^6$ Ω-cm or a bulk carrier concentration of $n \sim 2 \times 10^{11}$ cm^{-3}. These results are typical for undoped, magnetron reactive sputter deposited CdS. Surface carrier concentrations determined by Schottky barrier $1/C^2$ measurements vary from 5×10^{15} cm^{-3} to 5×10^{17} cm^{-3}. Bulk film carrier concentrations estimated from Schottky barrier forward resistance or measured by the van der Pauw technique range from $n \sim 10^{11}$ to 10^{13} cm^{-3}.

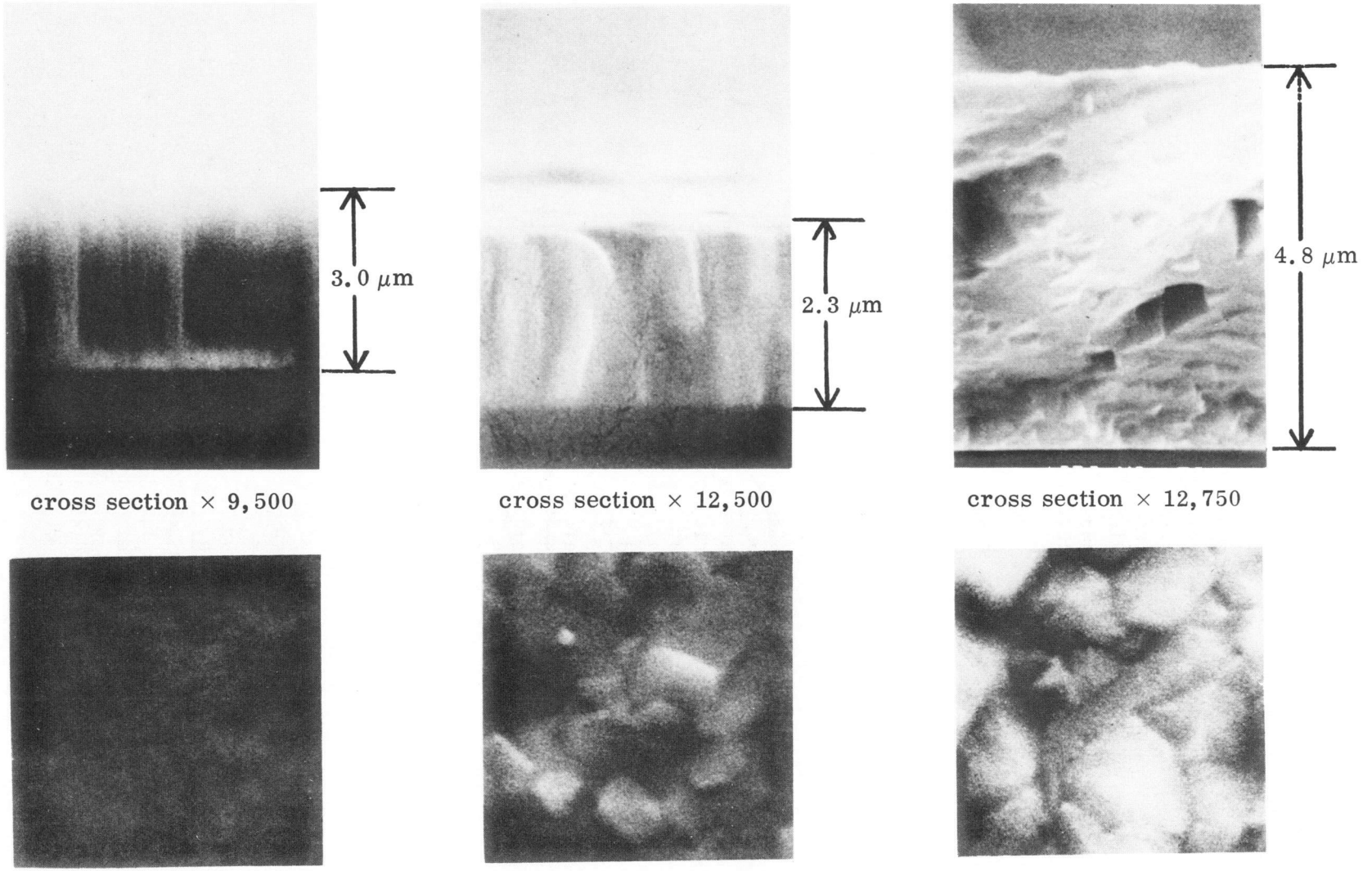

Fig. 8 SEM Photos of CdS Films Sputtered at Various H_2S Pressures onto Substrates at Constant Temperature, T_s = 300°C

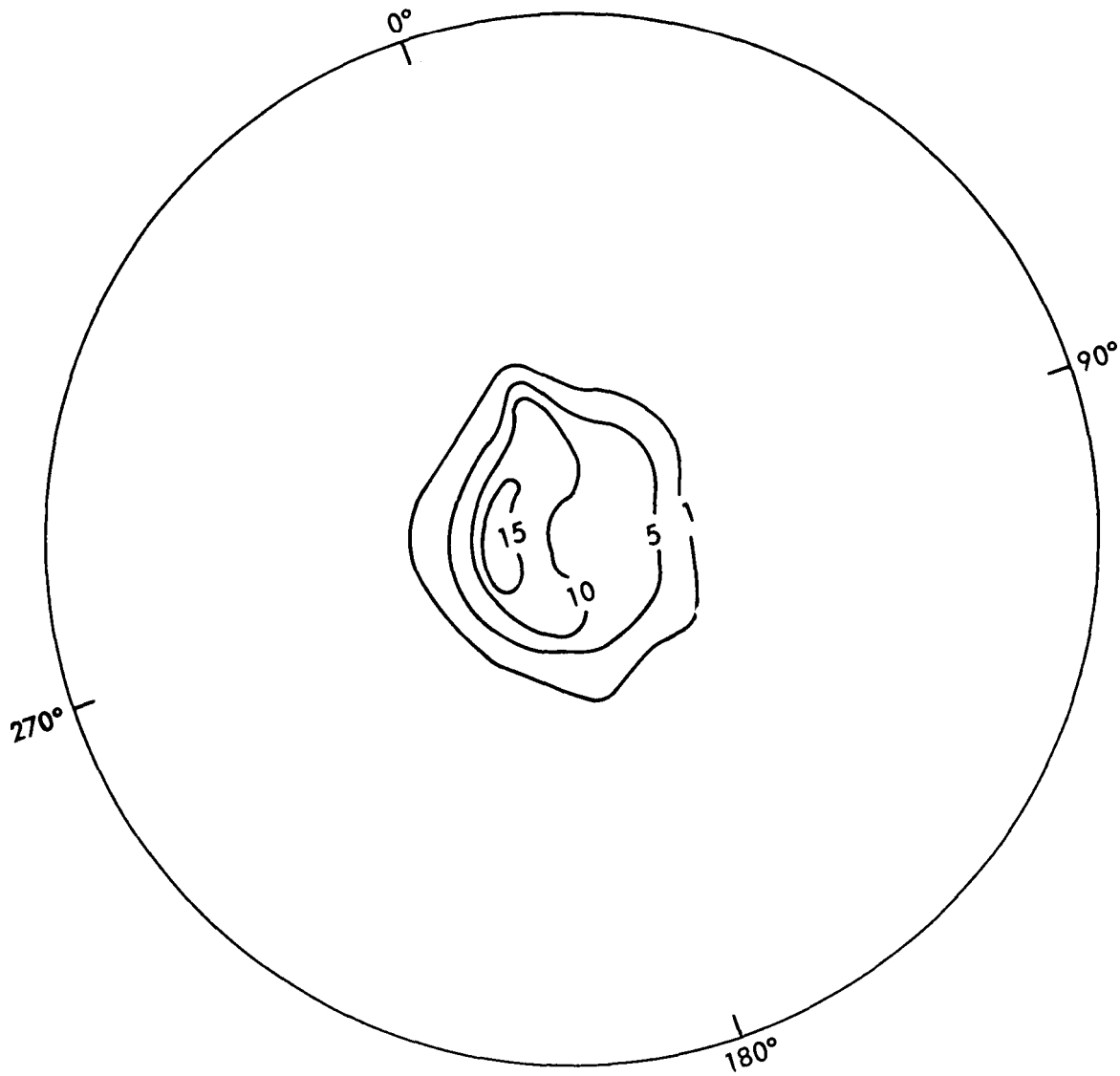

Fig. 9 Pole Figure for Distribution of 0001 Pole Density of CdS Film From Figure 8b. Numbers Represent Times Random

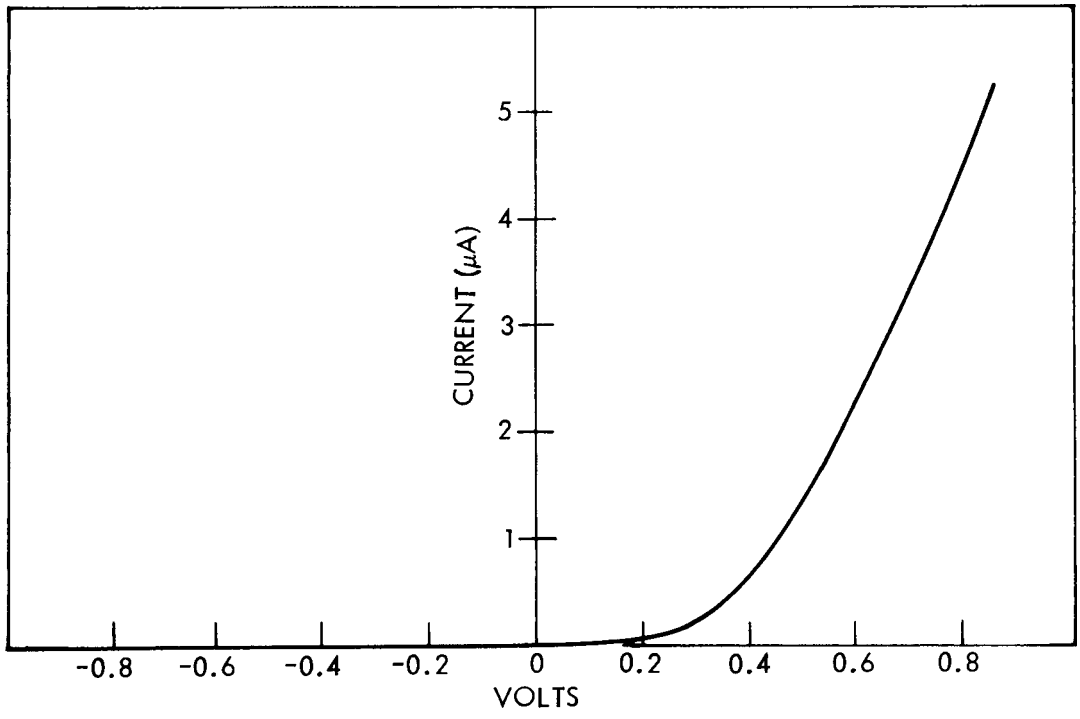

A. Au/CdS DIODE CHARACTERISTIC

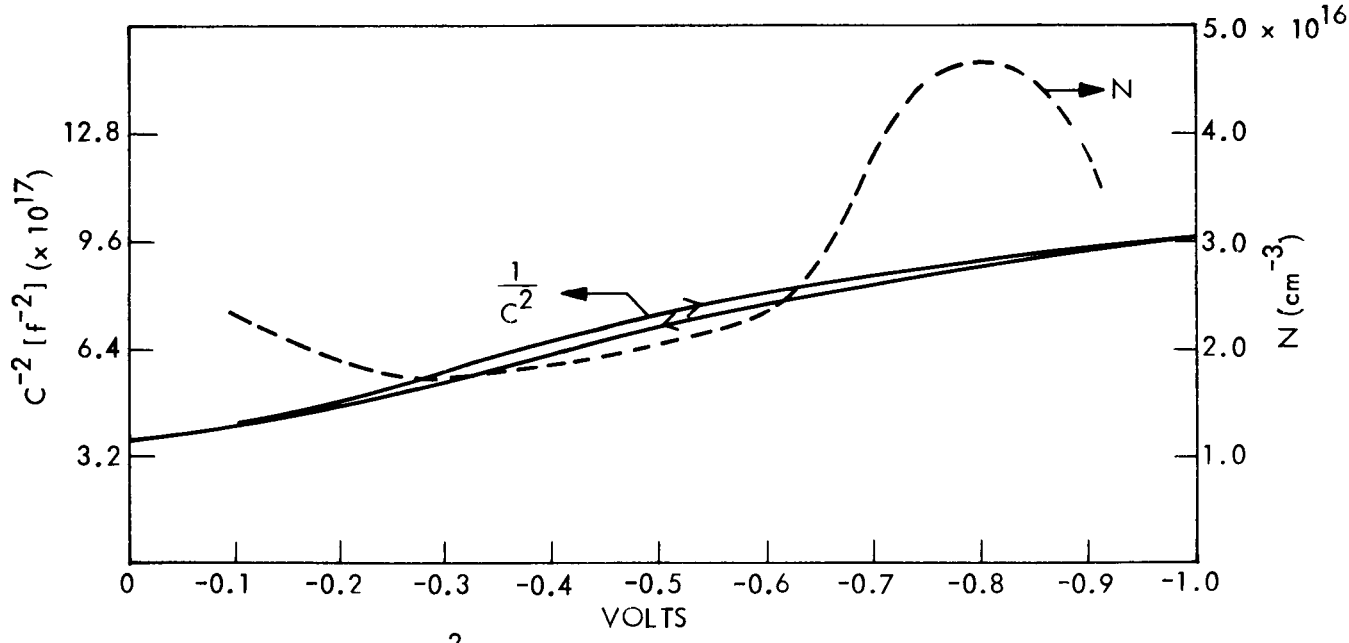

B. REVERSE BIAS $1/C^2$ VERSUS V AND CORRESPONDING CHARGE DENSITY

Fig. 10 Electrical Characteristics of Au Schottky Contact to Reactively Sputtered CdS Film

As discussed above with respect to Task 1.2, Deposition of $Cd_{1-x}Zn_xS$, reactive sputtering of CdS in H_2S results in a sulfur-rich or nearly stoichiometric composition. However, at the conclusion of a sputtering run, the H_2S flow is terminated and the substrate is slowly cooled from the deposition temperature ($T_s \approx 250^oC$) to room temperature. During this interval, S is lost from the surface of the film, resulting in a high conductivity surface layer. Changes in surface layer conductivity due to rapidly duffusing native defects at low temperatures ($T \approx 200^oC$) is a common observation in II-VI compounds in general [6] and in CdS in particular [7]. The significance of this observation is that reactively sputtered CdS films are amenable to carrier concentration and conductivity control. Film conductivity has also been increased by annealing in an H_2 ambient [8].

The capacitance measurement indicated in Figure 10b was performed with an ac voltage at 3.14 kHz. The capacitance is non-dispersive for signal frequencies from 800 Hz to 100 kHz. The loss tangent is only slightly dispersive. The junction formed by Au evaporated onto reactively sputtered CdS films is not modeled by either a simple series or parallel circuit. There is significant trapping and detrapping of charge in the space charge layer as indicated by 1) hysteresis in the C-V curve (see Fig. 10b), 2) significant hysteresis in the I-V curve when observed on a curve tracer (30 Hz rep. rate) and 3) the junction impedance characteristic noted above. Slow trapping and detrapping of charge will also be noted below in Task 1.9, Photovoltaic Barrier Measurements.

Task 1.6 Deposition of Cu_2S

In a previous study Cu_xS coatings were deposited onto glass substrates at various H_2S injection rates and substrate temperatures. The electrical and optical properties of the Cu_xS were found to depend on both of these parameters [5]. A series of Cu_xS coatings have been deposited over pre-deposited CdS (in the same pumpdown) using the Cu_xS conditions suggested by the results on glass. A consideration in making such coatings is that the substrate holder assembly has a relatively long thermal time constant. In particular the Cu_xS coatings were applied over CdS coatings that had been deposited at a substrate temperature of 220^oC. Two procedures were used in depositing the Cu_xS coatings: (1) the Cu_xS coatings were deposited quickly (about 4 min.) after conclusion of the CdS deposition and before the substrates had cooled to less than about 180^oC and (2) after the substrates had been allowed to cool to less than 50^oC (about 200 min.). Provisions are being made to shorten these times.

Task 1.7 Structural Measurements of Cu_2S

SEM surface measurements were performed on Cu_xS layers on CdS film substrates. Typically, the CdS topology was observed in Cu_xS covered areas due to the thin ($\sim$.15μm) layer of Cu_xS. Note that the surface roughness of the CdS films in Figure 8 is only the order of $\sim$.2μm. The most notable exception occurred when Cu nodules were formed during Cu_xS deposition. The Cu nodules were associated with high resistivity films as had previously been noted for Cu_xS deposited onto glass [1,9].

Task 1.8 Electrical Measurements of Cu_2S

Since the CdS film underlying the Cu_xS is semi-insulating, in the plane of film measurements were made on the Cu_xS between Au contact dots. Film resistivity was estimated assuming conduction between two circular contacts of radius, r, separated by a distance, 2d, in an infinite plane. Resistivity is then given by:

$$\rho = R \frac{\pi t}{\cosh^{-1}(d/r)} \quad \Omega\text{-cm}$$

where t is the film thickness and R is the measured resistance between contacts.

High resistivity ($\rho \sim 15$ Ω-cm) Cu_xS films were obtained when Cu nodules were present. Otherwise, Cu_xS film resistivities were very low ($\rho \sim 10^{-3}$ Ω-cm). Cu_xS film resistivity increased with H_2 heat treatment. Typically, a 10x increase in resistivity was observed after annealing a film for 6 hours at 200°C in an H_2 ambient. A tentative explanation is that excess S is removed as H_2S to drive Cu_xS (where $x < 2$) towards the stoichiometric Cu_2S.

Curve tracer measurements on both high resistivity and low resistivity films indicated that the evaporated Au contacts were ohmic.

Task 1.9 Photovoltaic Barrier Deposition

Referring to Figure 2, it is seen that the substrate holder has provision for mounting seven substrate wafers. Only the center three substrate positions are currently being loaded, since relatively short Cd sputtering targets are being used to reduce the target costs. Dummy substrates with attached thermocouples are mounted above and below the three central deposition substrates. The dummy substrates are used to provide measurements of the substrate temperatures.

Thus three CdS coatings in the form of a 1.9 cm disks are deposited over precoated rear electrodes on borosilicate plates during each pumpdown in the CdS material studies described above. A moveable shield arrangement has been added so that a Cu_xS coating can be deposited over a portion of at least one of the CdS coatings that are deposited during each pumpdown. Thus each CdS coating can be evaluated both for its own properties and for the properties of an associated heterojunction.

Most Cu_xS/CdS junctions formed to date have been characterized by a soft reverse breakdown characteristic and high forward series resistance as shown in Figure 11. The soft reverse breakdown is augmented by a photosensitive shunt resistance. The high forward series resistance is comparable to that

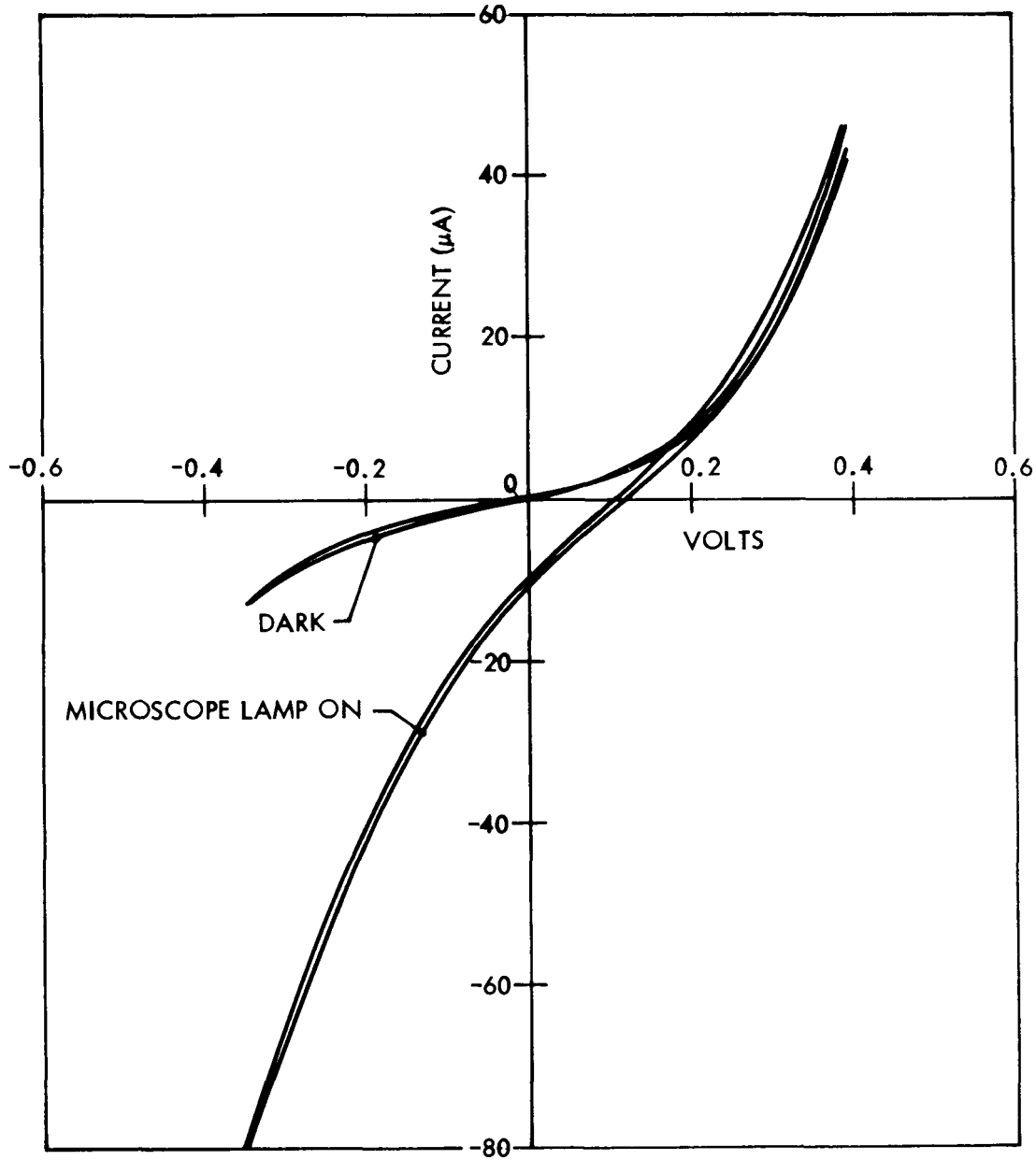

Fig. 11 Current-Voltage Characteristic of Reactively Sputtered Cu_xS/CdS Multilayer Film

observed for Schottky barrier diodes formed on CdS material deposited simultaneously with the material used for the photovoltaic junction measurements.

Open circuit photovoltages of 0.15 volts are typical. A short circuit current collection efficiency of $\eta \approx 0.1\%$ is typical in unannealed devices under .6328 μm irradiation. This is expected given the high surface doping and low bulk conductivity of the CdS films mentioned above in Task 1.5. Electrical Measurements of $Cd_{1-x}Zn_xS$. A simple expression for the current collection efficiency is derived in Task 3, Theoretical Analysis which shows the deleterious effect of the present resistivity variation of the CdS films:

$$\eta = \frac{.25\ \bar{\upsilon}_{th} \exp\ (-q\phi_B/kT)}{S + .25\ \bar{\upsilon}_{th} \exp\ (-q\phi_B/kT)}$$

Where ϕ_B is the potential barrier between the low and high resistivity CdS regions and S is an effective surface recombination velocity in the low resistivity layer. For $S = 10^6$ cm/sec., a potential barrier of 0.12 to 0.25 eV will give the low collection efficiencies observed. Thus, control of the conductivity profile of the CdS film layer is a crucial problem in obtaining efficient photovoltaic cell response.

Short circuit current response is quite uniform across the Cu_xS region of a cell as shown in Figure 12. A focussed He-Ne laser beam was scanned over the surface of the cell and the short circuit current simultaneously plotted on an x-y recorder. Dips in the response are due to shadowing of the laser beam by the Au contact dots indicated in the insert to Figure 12. Two features are of significance in Figure 12. First, the response on sweeps across the sample between Au dots show a slightly enhanced response near the edges (thinner regions) of the Cu_xS. This indicates that the Cu_xS absorption constant at .6328 μm and electron diffusion length are such that optimum response at .6328 μm occurs for Cu_xS thickness somewhat less than t = .15μm. With the known absorption constant at .6328 μm of 5×10^4 cm^{-1} [1] and a measurement of Cu_xS thickness as a function of position, it will be possible to deduce the electron diffusion length, L_n, in Cu_xS films from this type of measurement. Second, note that response to alternate sweeps are offset to the right or left. This is due to the slow photovoltaic response associated with deep level trapping and detrapping referred to above in Task 1.5 Electrical Measurements of $Cd_{1-x}Zn_xS$. The offset may be reduced by using slower scan speeds.

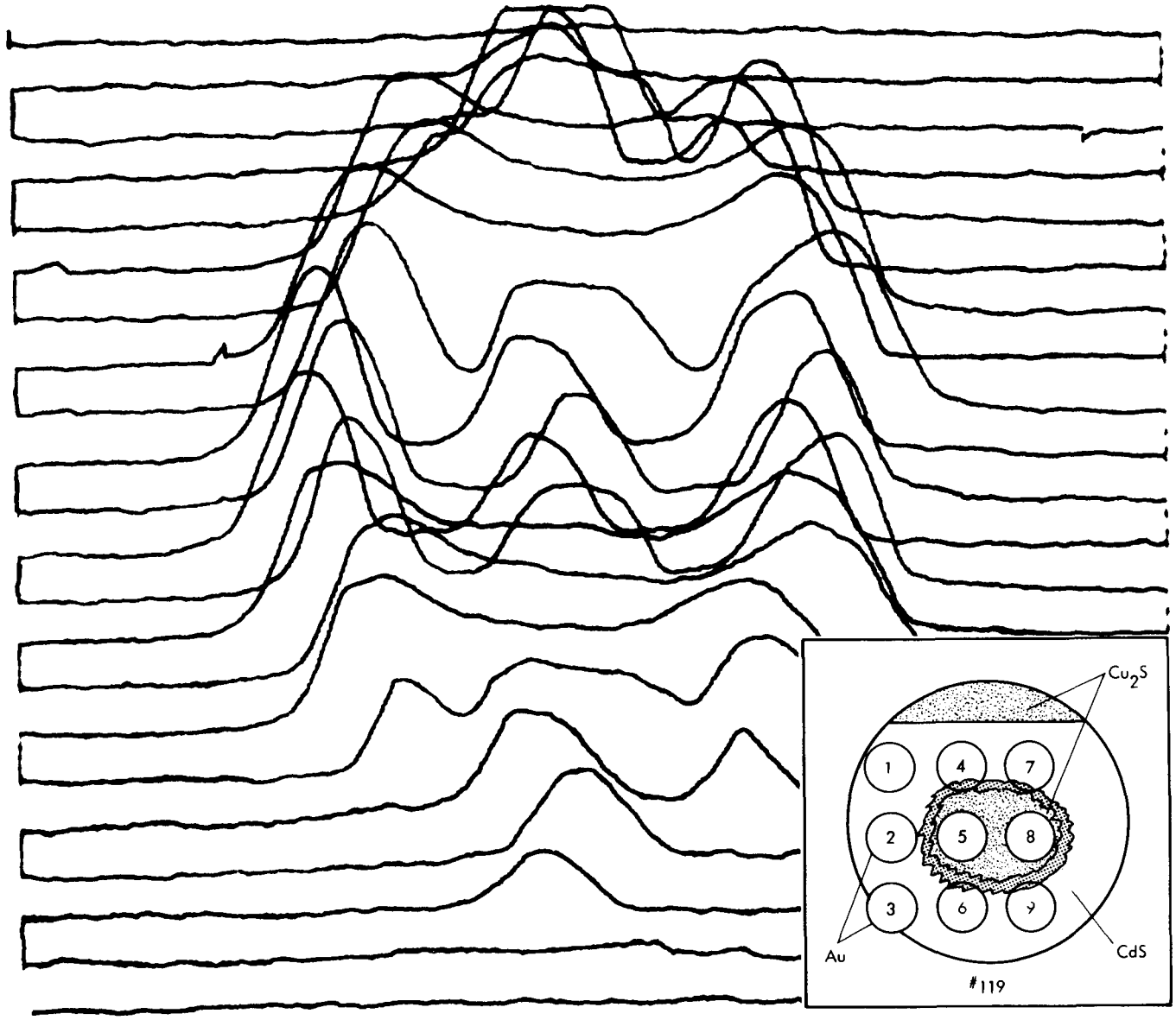

Fig. 12 Short Circuit Current Response Over Cu_xS Surface of Cu_xS/CdS Cell

Task 2.1 Au Grid Fabrication

The design of a first configuration for the top grid electrode has been established. An electroplated gold sputtering target and substrate holders with provisions for magnetic retention of deposition masks have also been prepared. The firm that had agreed to fabricate the magnetic masks has encountered difficulties because of the small sizes involved. The first approach was to use chem-milling. They are now examining electro-forming. It appears that there will be a delay before the fine-grid masks designed to provide near optimum efficiency will be available. Therefore the possibility of fabricating a less delicate mask by chem-milling for use in the interim is being explored. Such masks would allow test solar cells for evaluating material properties to be fabricated.

Task 2.2 ZnS Coating

Cominco American will begin fabrication of the 6-9's zinc sputtering target as soon as work is complete on the Cd-Zn target. When the zinc target is received the ZnS reactive sputtering studies will be started.

Task 3 Theoretical Analysis

The use of a built-in drift field is a well know technique to enhance the minority carrier diffusion length in solar cells. However, with the apparent doping distribution in the reactively sputtered CdS as prepared to date, the built-in field is such as to degrade cell performance. The proposed band structure as a function of position is indicated in Figure 13. The potential barrier between the highly conducting surface and semi-insulating bulk is given by

$$\phi_B = \frac{kT}{q} \ln \frac{n_{surf}}{n_{bulk}}$$

where n_{surf} is the free carrier density near the surface ($n_{surf} \approx 5 \times 10^{15}$ to 5×10^{17} cm^{-3}) and n_{bulk} is the free carrier density in the bulk of the film ($n_{bulk} \approx 10^{11}$ to 10^{13} cm^{-3}). If a photogenerated excess carrier density, n, is injected across the heterojunction into the CdS surface region, then, using a simple thermionic emission model for current flow across the nn^+-homojunction we find:

$$J_c = qn(1/4)\ \bar{v}_{th} \exp(-q\phi_B/kT)$$

for the collected current. The average electron thermal velocity is given by $\bar{v}_{th} = \sqrt{\frac{8kT}{\pi m_n^*}}$. A surface recombination velocity may be associated with

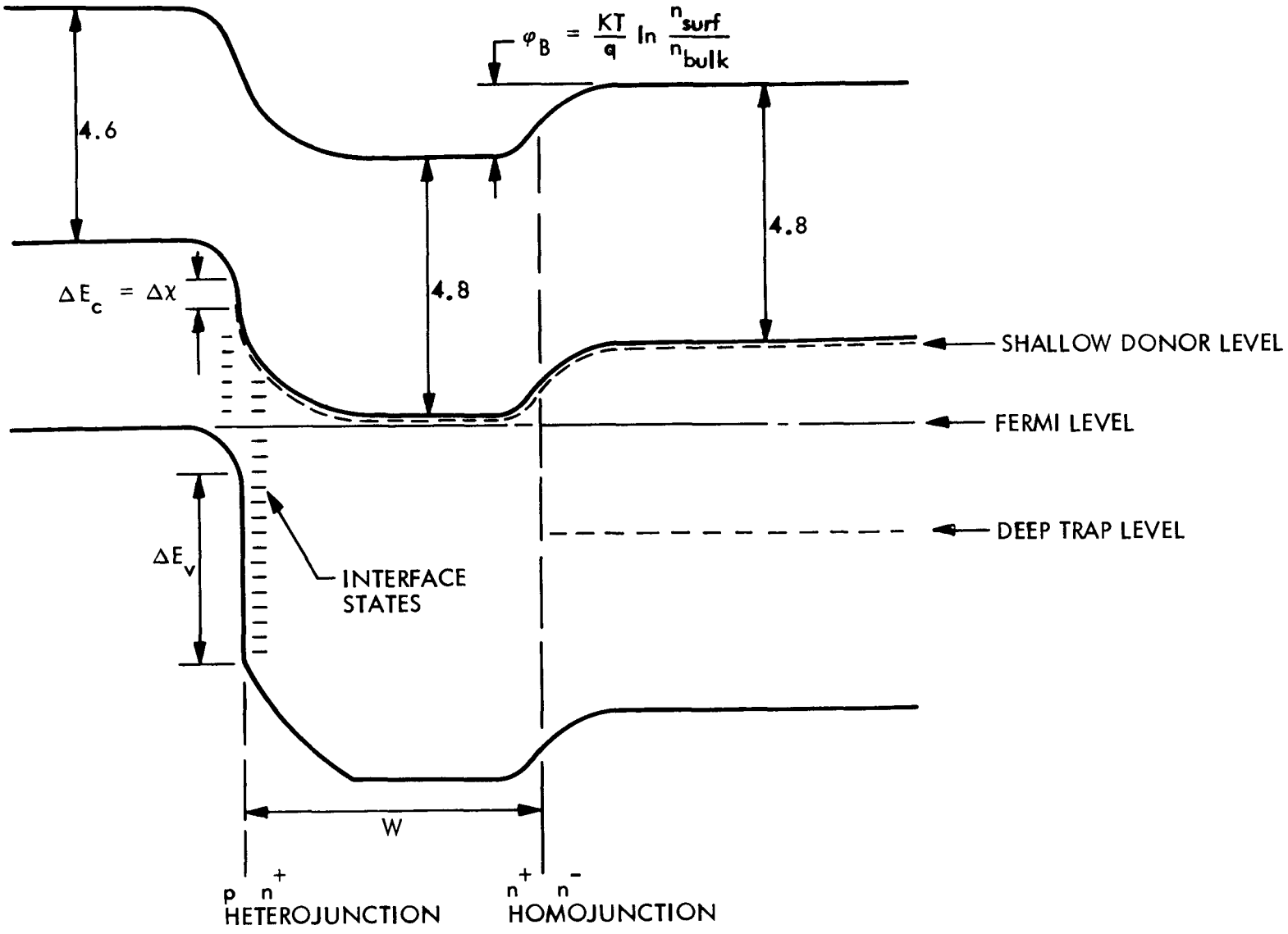

Fig. 13 Model of Heterojunction With Built in Retarding Field

the nn^+ homojunction interface so that a recombination current also flows:

$$J_R = qnS$$

where S is the homojunction recombination velocity. (An equivalent recombination velocity may be defined for bulk excess carrier recombination in the highly doped surface region of width, W. $S = \bar{\upsilon}_{th}\, \sigma\, N_R\, W$ where N_R is the density of recombination centers and σ is the capture cross section of a center.) The efficiency of external circuit photocurrent collection then includes a factor

$$\eta = \frac{J_C}{J_R + J_C} = \frac{.25\ \bar{\upsilon}_{th} \exp\ (-q\phi_B/kT)}{S + .25\ \bar{\upsilon}_{th} \exp\ (-g\phi_B/kT)} \quad .$$

It is obviously desirable to have a monotonically increasing free carrier density going from the Cu_xS/CdS heterojunction to the CdS/Substrate contact. This is partially accomplished in the conventional Cu_xS/CdS solar cell by the junction heat treatment step when some Cu is diffused from the Cu_xS into the CdS surface. In the reactively sputtered multilayer cell fabrication, deposition parameters will be programmed to yield the desired doping profile. Careful CdS or $Cd_{1-x}Zn_x$ resistivity control is a prime requirement for an efficient heterojunction solar cell.

Task 4 Conversion Efficiency

Optical measurments on Cu_2S films confirmed the applicability of Mulder's single crystal optical data [1]. Using an approximation to the solar photon spectral irradiance shown in Figure 14, the conversion and collection of photogenerated electrons in various thicknesses of Cu_2S was calculated from:

$$J_L = \bar{T} q\ 10^3 \int_{0.3}^{1.2} \phi(\lambda)\ \eta(\lambda)\ d\lambda \qquad mA/cm^2$$

where

$\bar{T} \approx 0.9$, average optical transmission into Cu_2S layer LMSC-Telic cell design

$\eta = \eta(\alpha\ (\lambda), L_n, t)$, internal quantum efficiency from Eqs. (2-9) or (2-10) of Ref. [10].

$\alpha(\lambda)$, Cu_2S absorption coefficient from Ref. [1 or 11].

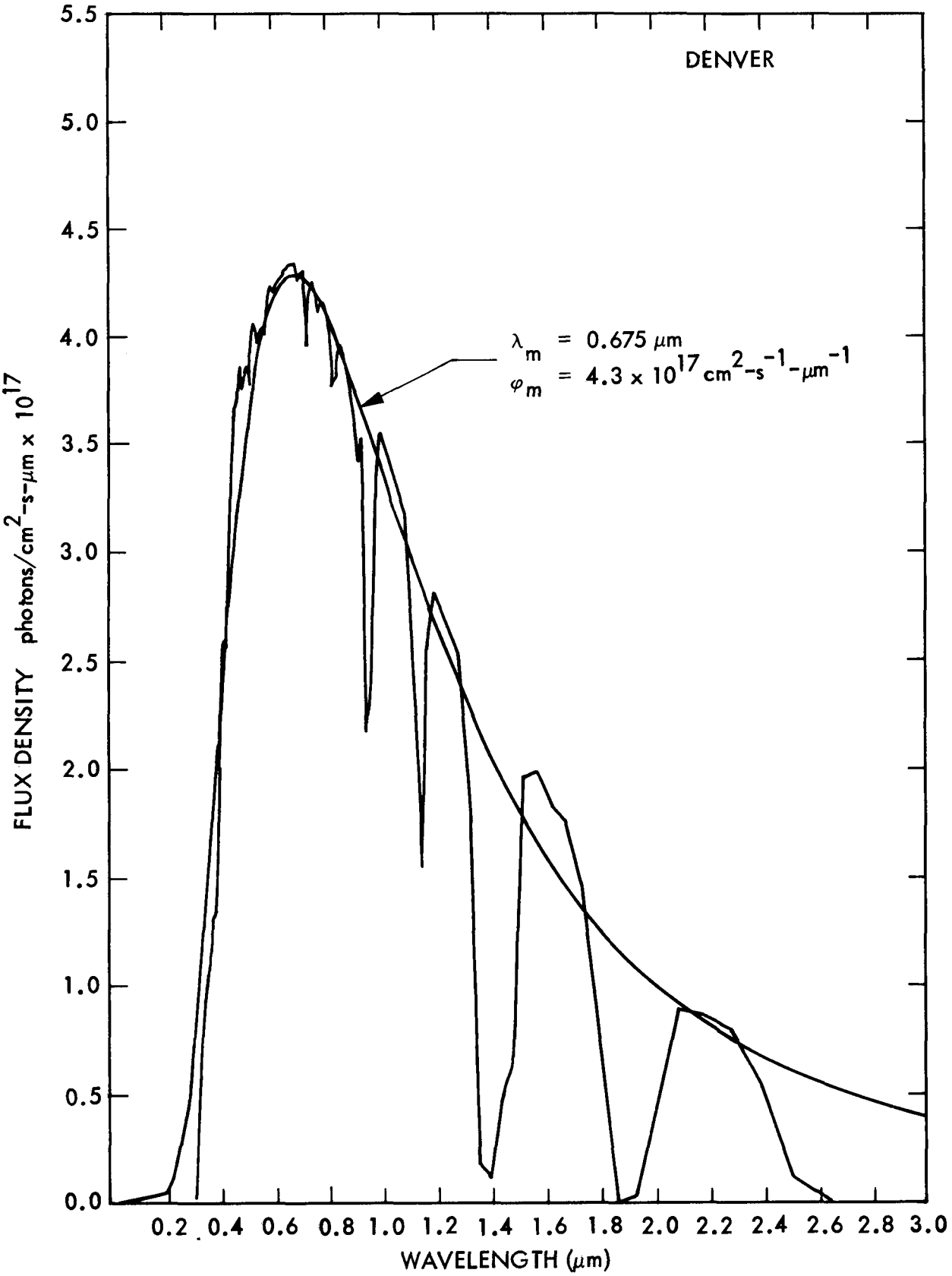

Fig. 14 Comparison of $\varphi(\lambda) = \varphi_m \lambda_m^4 (e^{3.92} - 1) / \lambda^4 (e^{3.92\,\lambda m/\lambda} - 1)$ Approximation to SOLTRAN Model

L_n , electron diffusion length in Cu_2S

t , thickness of Cu_2S layer

The collected photocurrent density is shown in Figure 15 for a reflecting back surface contact and in Figure 16 for a nonreflecting back surface contact. In both cases, a negligible Cu_2S front surface recombination velocity was assumed. The range of minority carrier diffusion lengths chosen is typical of those reported for Cu_2S [12]. A broad maximum in the optimum thickness of Cu_2S is found. The proposed design thickness of $t \approx 0.15\mu m$ is near optimum for a range of minority carrier diffusion lengths, $0.1 \leq L_n \leq 0.3\mu m$.

Three further conclusions on (Cd,Zn)S/Cu_2S cell development may be obtained from Figure 15. First, reports of $J_{sc} \approx 26$ mA/cm^2 (which was obtained on a textured surface and includes a small contribution from the CdS side of junction) [13] indicate that nearly ideal response is obtainable from the Cu_2S side of the heterojunction. Second, measured electron diffusion lengths $L_n < 0.1\mu m$ [14] are not representative of Cu_2S layers in cells with $J_{sc} > 20$ mA/cm^2. Finally, it is possible to obtain an estimate of ultimate power conversion efficiency in the (Cd,Zn)S/Cu_2S system as a function of open circuit voltage. In Figure 17 we show the output power of a cell based on the maximum photo currents in Figure 15 and assuming a fill factor, FF $\approx$ 0.8. Also shown in Figure 17 are the maximum open circuit voltages reported for CdS/Cu_2S and (Cd,Zn)S/Cu_2S cells [15]. From this, we may conclude that for a planar (Cd,Zn)S/Cu_2S interface, it will be necessary to utilize a (Cd,Zn) alloy which produces an open circuit voltage, $V_{oc} \approx 0.7$ V and improve the optical transmission into the cell to $T > 0.9$. In addition, comparison of Figures 15 and 16 indicates that a reflecting back contact surface is essential as well as a negligible Cu_2S front surface recombination velocity.

Task 5 Device Cost Projections

It is anticipated that the (Cd,Zn)S coatings will be used in fabricating (Cd,Zn)S/Cu_2S solar cells on glass substrates using the proposed LMSC solar cell configuration described in Ref. [10]. Production costs have been considered on the basis of an assumption that the cells will be produced at a rate to provide 1000 MW of new power generating capacity each year.
The following initial assumptions have been made:

- The peak solar flux will be 1 kW/m^2
- The solar cell efficiency will be 10%
- The production yield will be 75%
- Antireflection coating is not considered
- Costs in 1978 dollars

With these assumptions, the required yearly production would be 1.33×10^7 m^2/yr or 1.4×10^8ft^2/yr.

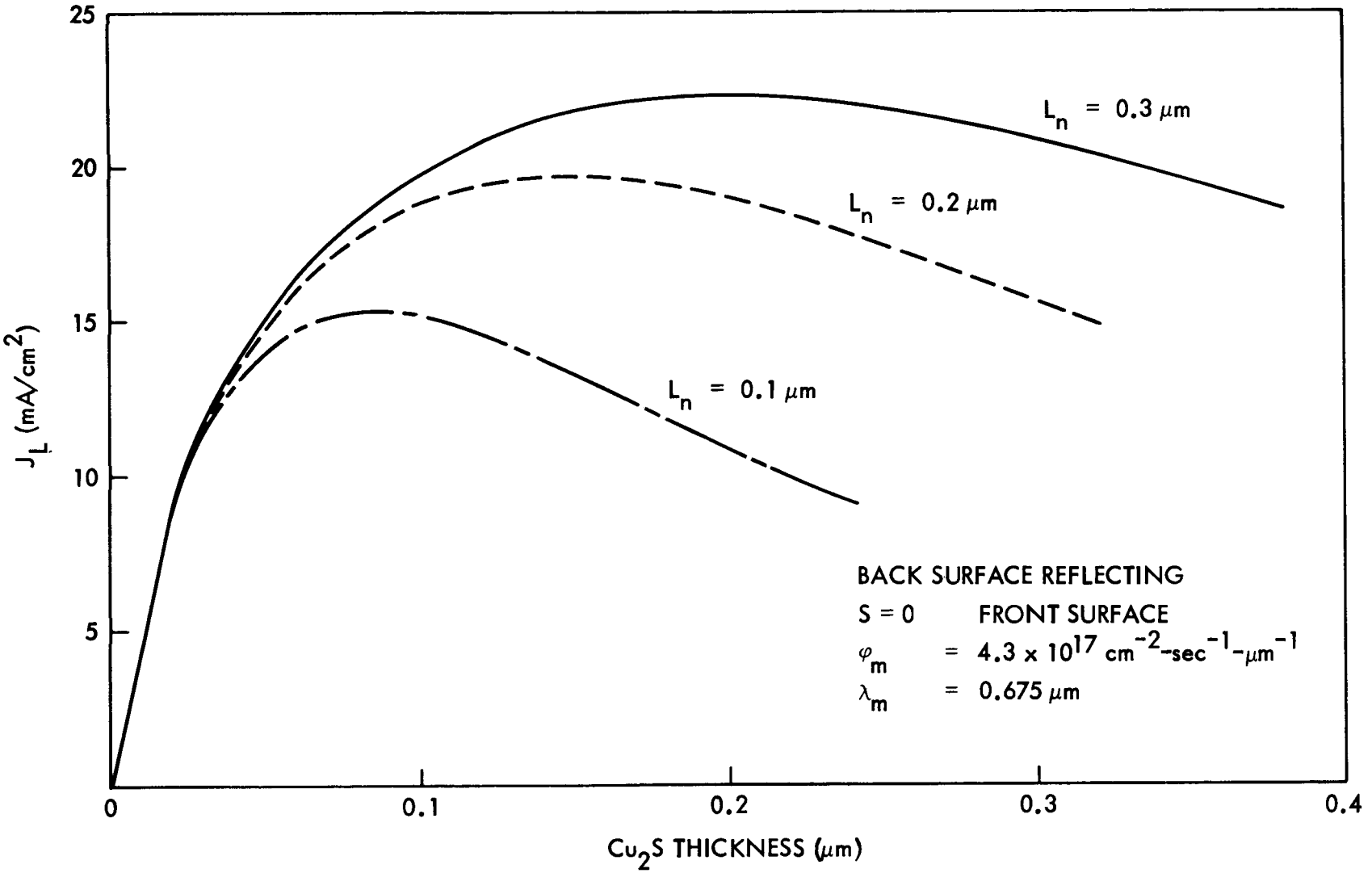

Fig. 15 Photogenerated Current in Cu_2S Side of (Cd, Zn)S/Cu_2S Solar Cell With Reflection From Back Surface of Cell. Assumed AMI spectral irradiance and S = O front surface recombination velocity

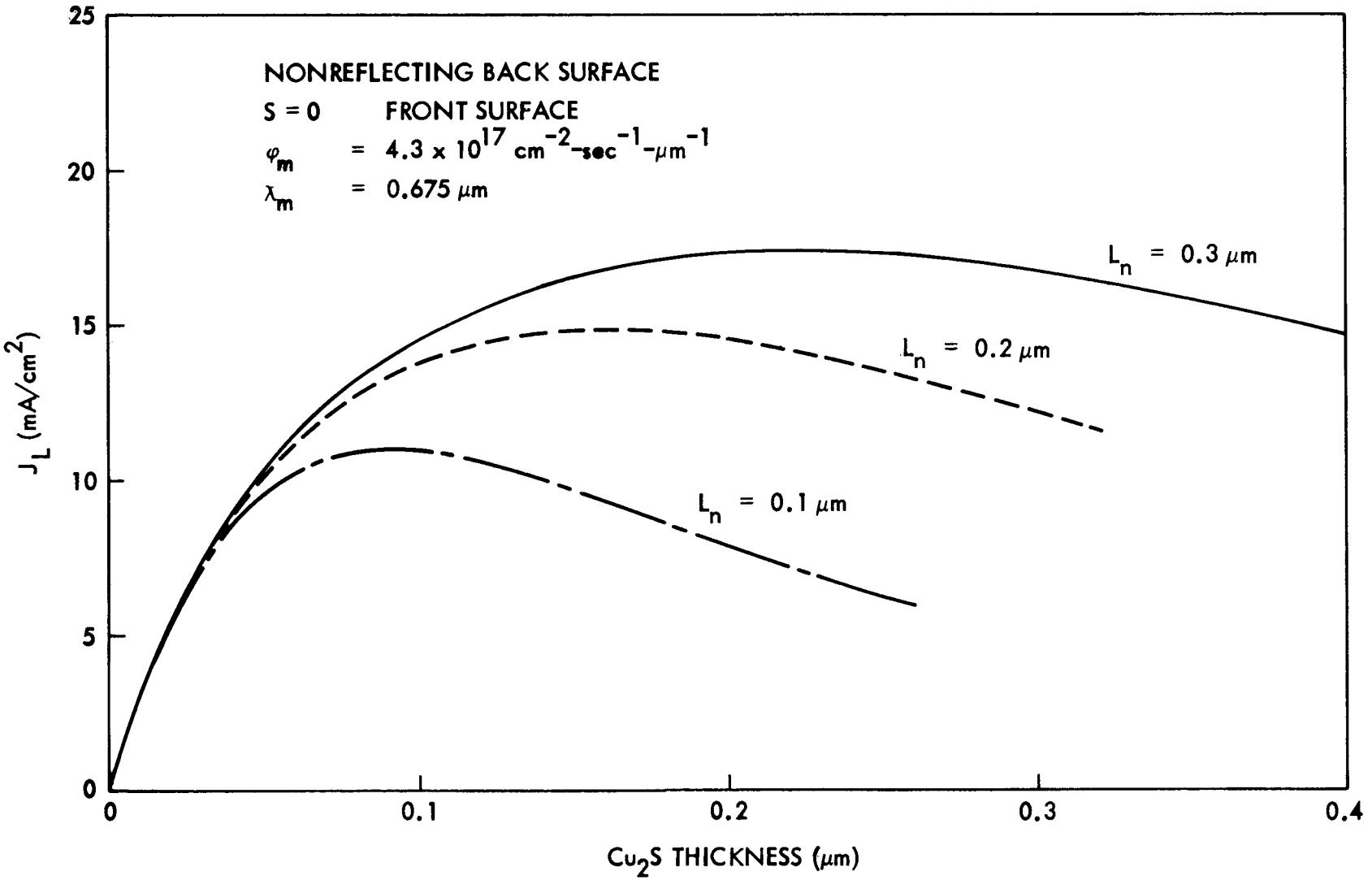

Fig. 16 Photogenerated Current in Cu_2S Side of (Cd, Zn)S/Cu_2S Solar Cell With No Reflection From Back Surface of Cell. Assumed AM1 spectral irradiance and S = O front surface recombination velocity

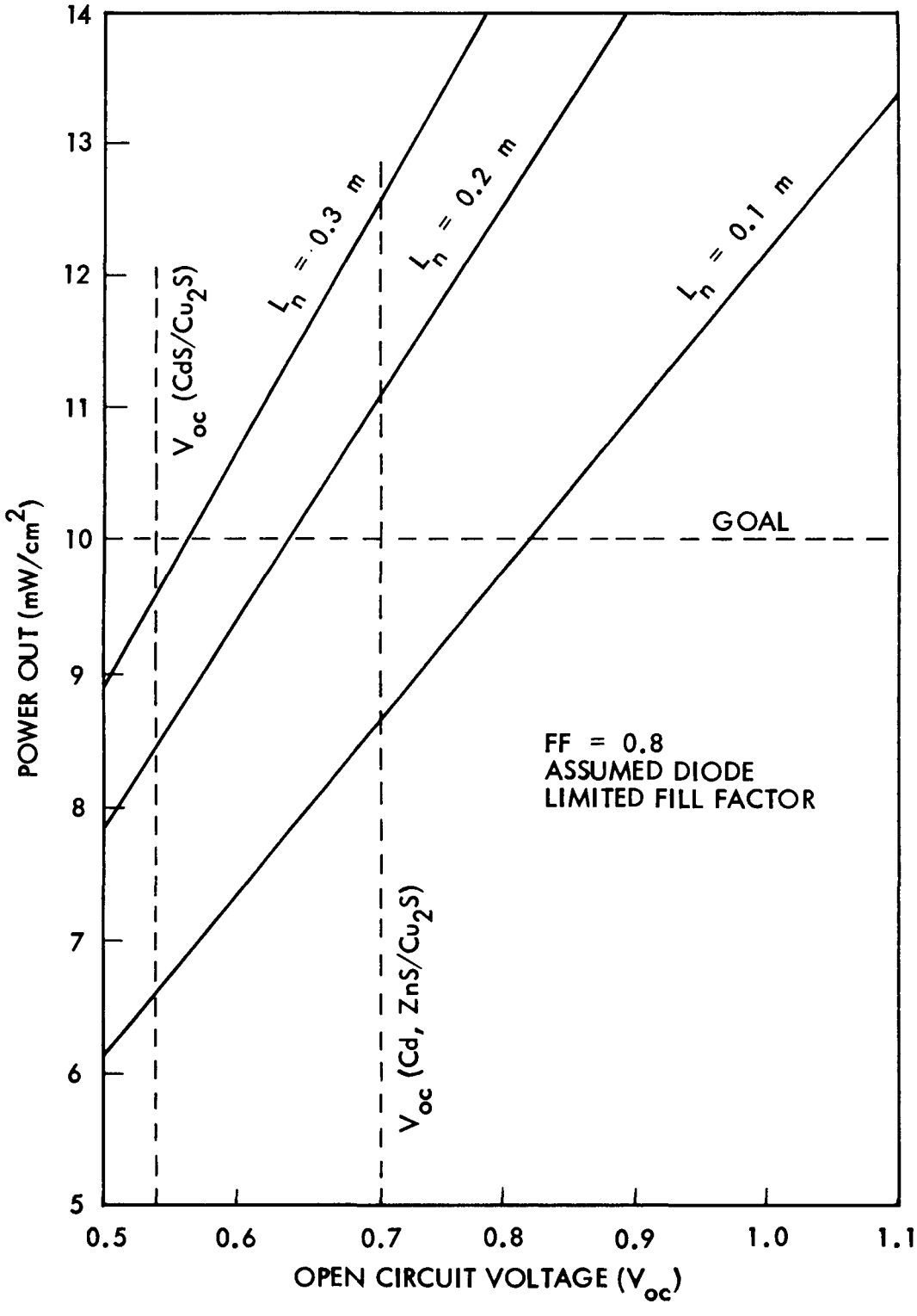

Fig. 17 Output Power of (Cd, Zn)S/Cu_2S Cell From Cu_2S Side of Junction. Calculation based on Figs. 2-19, 2-20, and 2-21 with additional assumption of a Fill Factor, FF = 0.8

First, cost of a CdS/Cu_2S solar cell produced entirely by Telic type post-magnetron sputtering is estimated since this process is of primary interest in the present program. The cost of adding Zn to the cell in forming (Cd,Zn)S tends to be compensated for by the reduction in the amount of Cd required. Thus, the CdS/Cu_2S cell cost analysis is a reasonable guideline, at this point, for estimating the $(Cd,Zn)S/Cu_2S$ cell costs. Also, the Cu required for the cell is negligible in amount and cost compared to Cd and thus can likewise be ignored. Based upon results to date it is estimated that the CdS layer should be about 3-um thick. The density of CdS is 4.8 g/cm^3. The mass of required coating is therefore 1.44×10^{-2} kg/m^2. Since the mass of the sulfur can be neglected, the cadmium requirement for the proposed production would then be 1.9×10^5 kg/yr (188 long tons/yr). The present price of 99.9999% (6-9's) cadmium in 100 kg quantities is about $125/kg. Cadmium is obtained primarily as a by-product of zinc and lead production. For large quantity usage, a moderate price reduction (e.g., to $100/kg) is projected. The cadmium material cost is then $1.44/$m^2$ or $0.14/$ft^2$.

For the post-magnetron reactive sputtering deposition method, the cadmium material must be cast into suitable cylindrical cathodes. The method has the advantage that a relatively small amount of coating material is lost (i.e., not applied to substrates).

However, a cost is associated with the casting process. From the experience gained by Cominco American in casting small-scale cathodes for this program, the production scale casting cost is estimated to be equal to the material cost in the case of 6-9's cadmium. This cost is then $0.14/$ft^2$.

A typical, medium-size, post-magnetron coating chamber could have a cylindrical substrate surface 1 m in diameter and 1 m in length. The range of deposition rates in the laboratory CdS, post-magnetron, reactive, sputteirng experiments was about 300 to 500 Å/min. Equipment modifications would allow this to be raised to 1500 Å/min. A rate of 1000 Å/min was conservatively assumed. The chamber residence time for depositing a 3-μm CdS coating is then 30 min. Thus, πm^2 of solar cell substrates are coated with CdS every 30 min in the "typical" chamber. If it is assumed that the machine operates, on the average, 80% of the time, the production volume for the CdS chamber is 0.08 m^2/min or 4.4×10^4 m^2/yr. The desired yearly production would then require about 250 machines. This is not an unusual requirement for a large production facility.

Laboratory post-magnetron Cu_2S reactive sputtering experiments were carried out at deposition rates comparable to that for CdS. Therefore, an in-line coating chamber identical to the CdS chamber could deposit 0.15-μm Cu_2S coatings without slowing the throughput. It is therefore assumed that there will be a continuous coating line consisting, for example, of seven in-line chambers, as follows:

(1) Input interlock chamber

(2) Base electrode deposition (through masks) chamber

(3) CdS deposition chamber

(4) Cu_2S deposition chamber

(5) Top electrode deposition chamber

(6) Heat-treat chamber

(7) Output interlock chamber

Each chamber will have a πm^2 substrate processing area. A cost of $175,000 each is assumed for the chambers (including vacuum pumping and substrate handling systems). A cost of $75,000 is added to each of the four coating chambers to cover the cost of power supplies and instrumentation. The total system cost, therefore, is about $1.5 million. If a 10-yr straight-line depreciation of the equipment cost is assumed, the result is an added cost to the solar cells of $\$3.41/m^2$ or $\$.31/ft^2$. (Engineering costs are not included in the equipment cost, since these would be averaged over the 150 to 250 such production units that would be required, and would make a negligible contribution.)

The production rate for the "reasonable apparatus" is about 1.0 ft^2/min. The apparatus will be highly automated. The primary labor requirments will be in cleaning the glass substrates (chemically) and loading and unloading the coating apparatus. It is estimated that two production units can be manned by a crew of seven - two for cleaning glass, two for loading the apparatus, two for unloading the apparatus, and one system operator. With the exception of the system operator, the crew can be virtually unskilled. A labor rate of $4/hr is assumed for the unskilled staff and $8/hr for the operator. With a 100% overhead (typical for a vacuum production operation), the labor cost is $32/hr or $\$.53/ft^2$.

The proposed solar cells are formed on glass substrates. Although actual glass costs are guarded by the glass industry, a large volume glass substrate cost of about $\$0.17/ft^2$ has been estimated by two presumably independent sources [16,17].

Other materials costs for production of the present-design cell are dominated by the gold gridding costs. Using 1978 prices of $200/Troy oz, and assuming 99% recovery of gold deposited onto the mask, it is estimated that an additional $\$7.20/m^2$ or $\$0.66/ft^2$ is required for a 5% area covering grid design of 2-μm thickness.

The CdS/Cu_2S solar cell production cost estimates for using a Telic type post-magnetron sputter deposition system are summarized along with the assumptions that were made:

o Labor	$0.53/ft^2
Six operators at $4/hr One operator at $8/hr } per two production units Overhead, 100%	
o Equipment	$0.31/ft^2
Basic unit cost, $1.5 million	
Production capacity, 4.8 x 10^5 ft^2/yr	
Straight line depreciation over 10 yr	
o Substrate (glass)	$0.17/ft^2
o Cadmium Material Cost	$0.14/ft^2
Based on $100/kg	
o Target casting cost, $100/kg	$0.14/ft^2
o Other Material (Au grid)	$0.66/ft^2
Total Production Costs	$1.95/ft^2
o Production fee	$0.59/ft^2
(30% before taxes)	$2.54
o Total Solar Cell Cost	$3.38/ft^2
(corrected for 75% yield)	

The power output from 10% efficiency solar cells is 0.1 kW/m^2 or 9.3 x 10^{-3} kW/ft^2. The estimated solar cell cost of $3.38/ft^2 then yields a cost of $363/peak kW (about $274/peak kW in 1975 dollars) including a 30% production fee.

Examining the scenario in more detail, it can be seen that the above costs are based on the use of in-line vacuum coating machines, each with a capacity of 4.4 x 10^4m^2/yr (4.8 x 10^5ft^2/yr) and costing about $1.5 million each. (An advantage in using machines of moderate but reasonable size is that engineering and shakedown costs become negligible. In addition, the increase in production capacity can be programmed by bringing new machines on-line according to a given schedule.) The required solar cell production capacity of 500 to 1000 MW per year would require the construction of 115 to 250 of these typical machines. Thus, for the 1000 MW case, the cost would be $375 million for an annual production capacity of 120 million ft^2 of solar cells. This seems reasonable since it has been noted that the cost of a sheet glass plant with an annual capacity of 400 million ft^2 was constructed at a cost of $80 million (Ref. [17], adjusted to 1978 dollars).

Finally, it should be emphasized that these costs are based upon results of the program to date. Economy measures will be explored in several areas. For example, if eventual cell fabrication can proceed with 5-9's cadmium material, material and cathode casting costs will be reduced to $\$0.06/ft^2$ each. Replacement of the Au grid by an Au/Cu grid deposition could reduce the "other materials" costs by $\$0.45/ft^2$. These two developments would reduce the cell costs by 31% to about \$250/peak kW (\$189/peak kW in 1975 dollars).

What is the energy required to fabricate a unit area of solar cell by cylinder-post magnetron reactive sputtering and how long must the cell operate at peak output power to repay this energy investment? In responding to this question we refer to the CdS layer deposition experience gained in the program to date. An 8-in. height x 1-1/2-in. diameter cylindrical cadmium cathode was used to deposit a 3-μm thick layer of CdS in 1 hr. 7 min. The current to the cathode was 1 A and the discharge voltage varied between 800 and 900 V. The total available coating area under these laboratory conditions is approximately 130 in^2. Thus, about 1 $kW\text{-}hr/ft^2$ is required for the CdS deposition. At 9.3×10^{-3} kW/ft^2 peak power output form a 10% cell, 107 peak hours cell operation are required to recoup the CdS deposition energy investment. This is less than a month of total operation time.

The main source of cadmium for all cadmium alloy products is the smelting and refining of zinc ores. The cadmium byproduct concentrates are in the form of fumes from zinc calcine sintering plants (pyrohydrometallurgical zinc refining) or precipitates from zinc electrolyte in electrolytic zinc refining. Details of the principal processing techniques and their environmental impact are given elsewhere [18,19] and will not be considered separately here because these emissions would exist whether or not cadmium was used as a byproduct for solar cells.

Table 1 summarizes the results of Gandel et al. [20] who have estimated the pollutants generated from the manufacture of 9000 peak MW/yr CdS solar cells. Two proposed production methods were investigated: (a) Front surface cells by spray deposition [21] and (b) Back surface cells by vacuum deposition [22]. Pollutant levels are compared to thoese produced by 9000-MW coal fired steam generators operating for 1 yr.

Table 1

PRIMARY AND SECONDARY POLLUTANTS* GENERATED FROM THE MANUFACTURE OF CADMIUM SULFIDE CELLS FOR 9000 MW/YEAR (PEAK)**

Pollutants	Front Surface Cells		Back Surface Cells	
	kg/yr	%†	kg/yr	%†
Air				
SO_2	6.9×10^6	2.4	7.6×10^6	2.7
Particulates	9.3×10^4	0.4	6.0×10^5	2.5
CO	0.4	Nil	0.5	Nil
Hydrocarbons	0.1	Nil	0.1	Nil
NO_2	1.2	Nil	1.5	Nil
Cd	5.2×10^2	120	6.3×10^2	146
Water				
Oil/Grease	5.6×10^3	1.8	5.0×10^5	164.4
As	5.5×10^1	0.04	6.1	Nil
Cd	1.1×10^2	1.1	1.3×10^2	1.3
Cu	1.4×10^1	3.9	1.5×10^1	4.2
P	2.0×10^2	0.1	1.8×10^4	9.1
Pb	–	–	0.6	Nil
Se	5.2×10^1	0.1	3.1×10^1	0.1
Zn	5.2×10^1	0.1	3.6×10^1	0.1
Solids				
CdO	1.6×10^2		1.9×10^2	
$ZnSO_4$	1.6×10^2		2.0×10^2	

*Excluding emissions from the raw cadmium feedstock (densified, cadmium rich fumes from zinc smelters) and primary emissions from cell surface processing.

**Equivalent to the production of 8820 MT of CdS for front surface cells and 7344 MT of CdS for back surface cells. This represents the demand, in the year 2000, from solar photovoltaic power plants producing 1% of the total U.S. demand for electricity (9000 MW).

†Emission as percentage of the corresponding rates emitted from coal-fired steam generators producing 9000 MW-yr of electricity in the year 2000, assuming application of New Source Performance Standards control technology.

SUMMARY

Two fabrication problems must be solved before solar cells with reasonable performance expectations can be fabricated: (1) the electrical resistance of the deposited CdS must be reduced, and (2) suitable masks must be procured for depositing the gold grid electrodes.

It is planned that indium doping will be used to obtain the desired conductivity in the CdS and $Cd_{1-x}Zn_xS$. Thus, a Cd-10% Zn sputtering target with 200 ppm In is being fabricated at Cominco American and should be delivered to Telic by the end of September. In the interim period co-deposition of In is being used to explore In doping in CdS coatings.

When the Cd-10% Zn target is completed, reactive sputtering studies using it will begin at Telic and Cominco American will start work on the Zn target required for the anti-reflective coating. By the time the Zn target is completed it is anticipated that the Telic $Cd_{1-x}Zn_xS$ studies with the doped target will have progressed to the point where the Zn and In compositions can be specified for a final target that is scheduled to be fabricated by Cominco American for the present program.

Electro-forming is being explored for fabricating the deposition masks. If a time delay is encountered, interim masks of a less detailed nature will be fabricated so that diagnostic solar cells (no anti-reflective coating) can be fabricated as soon as the desired CdS conductivity is achieved.

Electrical and photoelectronic properties of multilayer cells deposited to date have been rather poor. However, the basic mechanisms responsibile for the performance have been analyzed and appropriate corrective modifications of the reactive sputtering deposition process are being evaluated.

A paper describing the Cu_xS reactive sputtering deposition studies that were made using glass substrates has been accepted for presentation at the 25th National Symposium for the American Vacuum Society to be held in San Francisco in November.

ANTICIPATED ACTIVITIES DURING NEXT REPORTING PERIOD

1) Task 1.2 Deposition of $Cd_{1-x}ZnS$

The CdS reactive sputtering studies to deposit coatings with controlled resistivity will be continued. Non-stoichiometric deposits will be examined. However the primary emphasis will be on the use of In doping. Coatings will be deposited using Cd-Zn target with 10% Zn and 200 ppm of In doping. A second target with varied Zn and In composition will be prepared depending on the results of the first set of studies.

2) Task 1.3 Substrate Contact

All CdS coatings will be deposited over pre-deposited rear electrodes. Fresh surface layers of Al, In, or Zn will be deposited over the pre-deposited electrodes as part of the CdS deposition. Thus it is anticipated that the rear contact details will be worked out in the course of the $Cd_{1-x}Zn_xS$ material studies described under Task 1.2 above.

3) Task 1.6 Deposition of Cu_xS

Cu_xS coatings will be deposited under various conditions over at least one of the $Cd_{1-x}Zn_xS$ coatings which is deposited during each pumpdown of the $Cd_{1-x}Zn_xS$ material studies described under Task 1.2 above. Thus the properties of sputtered Cu_xS coatings deposited under various conditions onto sputtered CdS surfaces will be examined during the course of the $Cd_{1-x}Zn_xS$ materials studies.

4) Task 1.9 Photovoltaic Barrier Formation

The $Cu_xS/Cd_{1-x}Zn_xS$ interfaces formed as described in Item 3 above will provide a concurrent opportunity to evaluate the photovoltaic properties of the junctions. As the work proceeds specific junctions will be fabricated for purposes of studying and attempting to maximize the photovoltaic response.

5) Task 2.1 Au Grid Fabrication

Masks will be prepared for depositing the top grid electrodes. If delays are encountered in forming the fine grid masks, interim masks will be fabricated for use in applying grids to test-type solar cells. When the grids are available, test solar cells will be fabricated in the course of developing the grid deposition technique.

6) Task 2.2 ZnS Coating

Cominco American is scheduled to deliver the Zn sputtering target during the next quarter. ZnS coatings will then be deposited for evaluation of their optical properties in anticipation of forming anti-reflection coatings on the solar cells.

REFERENCES

1. Technical Progress Report No. 3, Cadmium Sulfide/Copper Sulfide Heterojunction Cell Research, Lockheed Missiles and Space Company, LMSC-D626523 (30 June 1978)

2. J. A. Thornton, Ann. Rev. Mater. Sci. 1, 239 (1977)

3. H. W. Wieder, Intermetallic Semiconducting Films, Pergamon Press, N. Y. (1970)

4. L. R. Shiozawa, F. Augustine, G. A. Sullivan, J. M. Smith III, and W. R. Cook, "Research on Mechanism of Photovoltaic Effect in High Efficiency CdS Thin Film Solar Cells," Aerospace Research Laboratories, Rept. ARL 69-0155 (Oct. 1969)

5. Technical Progress Report No. 2, Cadmium Sulfide/Copper Sulfide Heterojunction Cell Research, Lockheed Missiles and Space Company, LMSC-D623523 (31 March 1978)

6. H. H. Woodbury, Physics and Chemistry of II-VI Compounds, ed, by M. Aven and J. S. Prener (North-Holland Publishing Co., Amsterdam, 1967) p. 248

7. R. Hill and I. A. S. Edwards, Vacuum, 27, 277(1977)

8. Technical Status Report No. 09 on DOE Contract EG-77-C-03-1459, Lockheed Missiles and Space Company, July 14, 1978

9. A. D. Jonath, W. W. Anderson, J. A. Thornton, and D. Cornog, "Copper Sulfide Films Deposited by Cylindrical Magnetron Reactive Sputtering," Proceedings 13th Photovoltaic Specialists Conference, Washington, D. C., (June 1978)

10. Cadmium Sulfide/Copper Sulfide Heterojunction Cell Research, Vol. I, Technical Proposal, LMSC-C084823 (June 1977)

11. B. J. Mulder, Phys. Status Solidi (a) 13, 79 (1972)

12. J. J. Oaks, J. G. Greenfield, and L. D. Partain, J. Appl. Phys. 48, 2548 (1977)

13. Institute for Energy Conversion, Semi-Annual Report EG-CC-7-03-1536-1, May 1978

14. J. Dieleman, NSF Conference on Cadmium Sulfide Solar Cells and Other Abrupt Heterojunctions, U. of Delaware, 92 (1975)

15. Institute for Energy Conversion, Final Report E(49-18)-2538 FR77, Nov. 1977

16. J. Harvey and J. Corkhill, Thin Solid Films 6, 227 (1970)

17. J. A. Thornton, J. Vac. Sci. Technol. 12, 830 (1975)

18. "Background Information for New Source Performance Standards: Primary Copper, Zinc and Lead Smelters, Vol. 1," EPA 450/2-74-002A, USEPA, Research Triangle Park, N.C., 1974

19. R. J. Nerkervis and J. B. Hallowell,"Metals Mining and Milling Process Profiles With Environmental Aspects," EPA 600/2-76-167, USEPA, Research Triangle Park, N.C., 1974, pp. 155-165

20. M. C. Grandel, P. A. Dillard, D. R. Sears, S. M. Ko, and S. V. Bourgeois, "Assessment of Large-Scale Photovoltaic Materials Production," EPA/600-7-77-087, Lockheed Missiles and Space Company, Inc., Huntsville, Ala.

21. J. F. Jordan, "Low Cost CdS/Cu_2S Solar Cells by the Chemical Spray Method," Proc. 11th IEEE Photovoltaic Specialists Conf.,1975, p 508

22. T. P. Brody and F. O. Shirland, "Prognosis for CdS Solar Cells," Symposium on the Material Aspects of Thin Film Systems for Solar Energy Conversion, May 1974

☆U.S. GOVERNMENT PRINTING OFFICE: 1979-640-258-1609